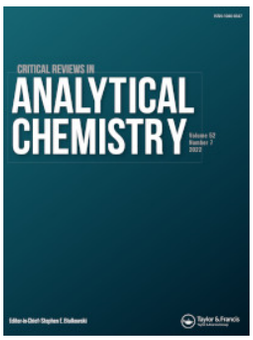

Taylor & Francis
Taylor & Francis Group

Critical Reviews in Analytical Chemistry

ISSN: (Print) (Online) Journal homepage: https://www.tandfonline.com/loi/batc20

An Overview of Aptamer-Based Sensor Platforms for the Detection of Bisphenol-A

Mustafa Oguzhan Caglayan, Samet Şahin & Zafer Üstündağ

To cite this article: Mustafa Oguzhan Caglayan, Samet Şahin & Zafer Üstündağ (2022): An Overview of Aptamer-Based Sensor Platforms for the Detection of Bisphenol-A, Critical Reviews in Analytical Chemistry, DOI: 10.1080/10408347.2022.2113359

To link to this article: https://doi.org/10.1080/10408347.2022.2113359

CRITICAL REVIEWS IN ANALYTICAL CHEMISTRY
https://doi.org/10.1080/10408347.2022.2113359

An Overview of Aptamer-Based Sensor Platforms for the Detection of Bisphenol-A

Mustafa Oguzhan Caglayan[a], Samet Şahin[a], and Zafer Üstündağ[b]

[a]Department of Bioengineering, Bilecik Şeyh Edebali University, Bilecik, Turkey; [b]Department of Chemistry, Kütahya Dumlupınar University, Kütahya, Turkey

ABSTRACT

Endocrine disruptive compounds are natural or anthropogenic environmental micropollutants that alter the function of the endocrine system ultimately damaging the metabolism. Bisphenol A (BPA) is the most common of these pollutants and it is often used in epoxy coatings and polycarbonates as a plasticizer. Therefore, monitoring BPA levels in different environments is very important and challenging. In recent years, an increasing number of BPA detection methods have been proposed. This article presents a critical review of aptamer-based electrochemical, fluorescence-based, colorimetric, and several other BPA detection platforms published in the last decade. Furthermore, a statistical evaluation has been made using principle component analysis showing analytical performance parameters do not create very different clusters. Comparisons to other BPA detection methods are also presented so that the reader has an overall literature overview.

KEYWORDS

Bisphenol A; endocrine disruptive compounds; aptamers; biosensor

Introduction

In recent years there has been a growing concern about receiving environments contaminated with various endocrine-disrupting compounds (EDCs). EDCs are substances that affect the endocrine system and the metabolism of steroid hormones.[1] EDC exposure causes obesity, diabetes, and cardiovascular diseases and increases the risk of cancer and neurotoxicity.[2,3] Therefore, EDCs can be called environmental pollutants, either naturally or anthropogenically.[4] An increasing number of studies have reported adverse effects of 800 different EDCs on human and wildlife health.[5,6] EDCs were also classified as chemicals of concern, for which restrictions on their usage continue to be imposed.[7] However, the detection of these EDCs, which have very low molecular masses, is challenging.[8,9]

Bisphenols (BPs) are well-known EDCs containing two hydroxyphenyl groups and there are more than fifteen BP analogs. The chemical structures of various BPs are summarized in Table 1. BPs are popular members of EDCs because they are used as plasticizers in the production of epoxy coatings and polycarbonate. Its presence in commonly used materials such as epoxy coatings (bottle caps, metal can and can liners, food packaging, etc.) and rigid transparent containers (water bottles, etc.) increases the risk of contamination posed by BPs.[19,20] Migration of BPs from food contact materials into foodstuffs results in increased exposure in humans. Studies have been conducted on the negative effects of BPs on human health and the environment, and especially regulatory organizations are conducting new studies on this subject.[21,22]

Bisphenol A (BPA) is one of the most widely used BPs and it has strong endocrine-disrupting effects.[10] Many studies have been reported focusing on the effects of BPA on human health, such as reproductive damage, and neural and behavioral disorders.[23,24] The effect of BPA on the endocrine system occurs through its binding to estrogen receptors.[25] Therefore, it has been reported to cause a decrease in sperm quality in humans[26,27] and to cause reproductive abnormalities in wildlife.[28] It has also been reported that even at low concentrations, BPA has the potential to induce chronic diseases and various types of cancer using in vitro animal models.[29–31] There is also a study in the literature showing that BPA can mimic the effect of thyroid hormone.[32]

In addition, since BPA is used as a plasticizer in a wide variety of food storage and packaging materials, migration of BPA to food products in food processes (heating processes such as pasteurization, sterilization, and canning) is important in terms of contamination.[33,34] BPA is also used in the production of phenoplast, phenolic and unsaturated polyester resins, polyvinyl chloride, and thermal paper.[35] BPA contamination in the range of 61 nM to 2.3 µM has been reported in water and food samples.[36–38] BPA was detected at nM-μM concentrations in environmental sources, such as wastewater,[39] river water,[40] sewage waters,[41] and surface waters.[42] Therefore, there is increasing attention to the detection of BPA in environmental water sources. Small amounts of BPA are discharged into wastewater

CONTACT Mustafa Oguzhan Caglayan oguzhan.caglayan@bilecik.edu.tr Department of Bioengineering, Bilecik Şeyh Edebali University, 11230 Bilecik, Turkey.

Table 1. Chemical formula and structure of BPA and its analogs.

BPA substitutes	Structure	References
Bisfenol A (BPA), 2, 2-bis (4-hidroksifenil) propan	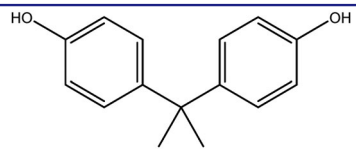	[10]
BPB, 2,2-bis (4-hydroxyphenyl) butane)	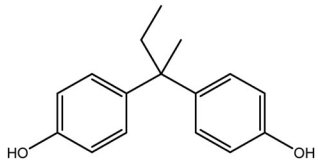	[11]
BPS, 4,4′ -dihydroxy diphenyl sulfone	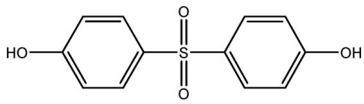	[12]
BPAF, 1,1,1,3,3,3-hexafluoro-2,2-bis (4-hydroxyphenyl) propane	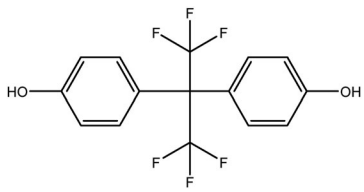	[13]
BPF (4, 4′ – dihydroxydiphenyl – methane)	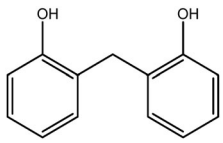	[14]
BPA-DGE (4,4′-isopropylidenediphenol diglycidyl ether)	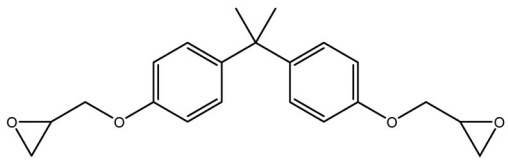	[15]
BPAP (4,4′-(1-phenylethylidene) bisphenol)	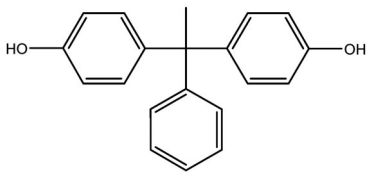	[16]
BPBP (bis(4-hydroxyphenyl) diphenylmethane)	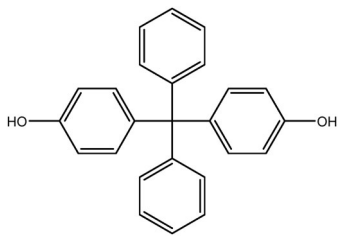	[16]
BPC (2,2-bis(4-hydroxy-3-methylphenyl) propane)	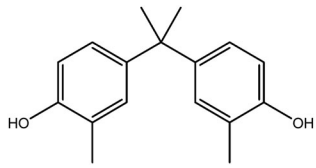	[16]

(*continued*)

Table 1. Continued.

BPA substitutes	Structure	References
BPC-dichloride = 1,1-dichloro-2,2-bis(4-hydroxyphenyl) ethylene	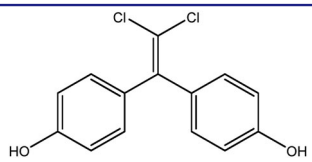	[15]
BPE 4,4′-ethylidenebisphenol	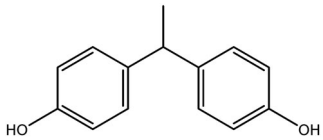	[16]
BPG 2,2-bis(4-hydroxy-3-isopropylphenyl) propane	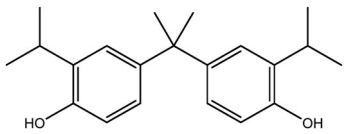	[15]
BPM = 4,4′-(1,3-phenylenediisopropylidene) bisphenol	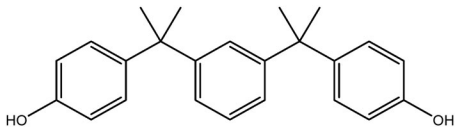	[15]
BPP = 4,4′-(1,4-phenylenediisopropylidene) bisphenol	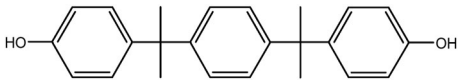	[17]
BPPH = 2,2-bis(2-hydroxy-5-biphenylyl) propane	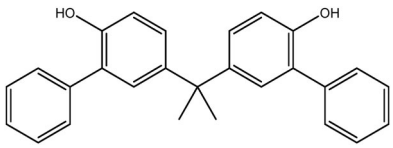	[15]
BP-TMC = 1,1-bis(4-hydroxyphenyl)-3,3,5-trimethylcyclohexane	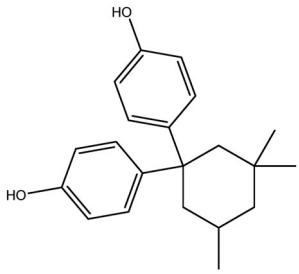	[15]
BPZ = 4,4′-cyclohexylidenebisphenol	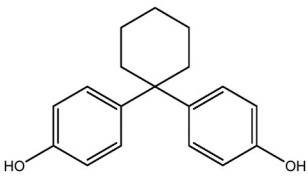	[18]

treatment plants after entering the environment from production and processing plants. BPA removal can occur in water treatment plants. However, it has been reported that water treatment technologies remove 76–99% of the BPA content in the source water only when granular activated carbon/UV exposure is used.[43] However, with this improvement, it is not sufficient to reduce BPA, which is found to be between 1.5 µM and 2 µM in 17% of the surface spring waters,[44] to 22 nM in the treatment facilities.[45]

Because of this obvious risk, many regulatory organizations banned the use of BPA and limited the specific migration limit of BPA in potential products to 0.05 mg/kg.[46] After the introduction of strict regulations on the production and use of BPA, derivatives such as bisphenol B (BPB),[47] bisphenol S (BPS),[48] bisphenol AF (BPAF),[13] and bisphenol F (BPF)[14] began to be used as alternatives to BPA (Table 1). However, since BPA analogs have a similar structure, it has been reported that these chemicals also show EDC behavior.[49,50] Similar to BPA, analogs have been reported to raise suspicion about reproductive disorders,[50,51] neurological problems,[52] cancer potential,[50,53] and metabolic disorders.[54] There are studies on the presence of some of these analogs (e.g., BPB) in food samples up to 277 nM.[19,55] Major analytical approaches for BPA

detection are based on methods such as liquid chromatography,[29,56] high-performance liquid chromatography (HPLC),[27,32] HPLC-mass spectrometry (HPLC-MS),[57] gas chromatography (GC),[58] and GC-MS.[30] Although these analytical methods are highly sensitive and accurate, most require expensive instruments and time-consuming sample pretreatment.[59] Therefore, in recent years, studies on the development of a portable, easy-to-use, cost-effective, and versatile detection strategy such as spectrophotometry,[19] immunoassay,[60,61] capillary electrophoresis,[62] fluorimetry,[63,64] and electrochemical detection[65] methods have attracted great interest in the literature.

Biosensors are suitable candidates for the detection of pollutants such as BPA, as with many analytes, with the advantage of selectivity provided by bio-recognition elements. The use of biosensors with high analytical performance in the detection of various chemicals in aqueous media has gained importance with the use of bio-recognition elements and nanomaterials such as aptamers, enzymes, antibodies, and whole cells.[19,63] However, due to the nonspecific affinity of immunoassays to BPA analogs (BPB or others),[66–68] aptamers have become an important biorecognition element for analytes such as BPA in recent years.[60]

Single-stranded (ss) DNA oligonucleotide aptamers are selected from specific oligonucleotide libraries ($\sim 10^{12}$–10^{14} unique oligonucleotide sequence) to bind to a target with high sensitivity and either high selectivity or general selectivity.[36] ssDNA aptamers are selected by exponential enrichment by a process called Systematic Evolution of Ligands (SELEX).[69–71] Aptamers have several advantages over other biodiagnostic elements: (i) more accurately distinguish functional groups between similar structures,[72] (ii) aptamers targeting small molecules can be selected *in vitro*,[73] and (iii) have a high affinity for their targets,[74] and (iv) it can be synthesized in large quantities *in vitro* and has the characteristics of simple preparation, easy acquisition, low cost, and easy storage.[75] In summary, the SELEX procedure is based on the interaction of the library with the analyte and the removal of low-affinity sequences until affinity in the micro-molar (μM) to nano-molar (nM) range is achieved.[76–78]

This cyclic separation and polymerase chain reaction (PCR) process are continued for 8–15 rounds.[79] In the SELEX process, the selectivity of the aptamer can be increased by removing sequences with counter-affinity for target analogs.[80,81] Affinity (K_d, dissociation constant) is used as a sensitivity scale.[72] SELEX methods such as FluMag SELEX,[82] Capillary Electrophoresis-SELEX (CE-SELEX),[83,84] and Graphene Oxide SELEX (GO-SELEX)[85] have also been developed to reduce the number of selection cycles or increase the efficiency and convenience of selections. As may be used of choice, sometimes aptamers are altered by truncation[86] and mutation.[87] There are reports of unchanged or increased affinity in this alternative modification.[86,88,89] The aptamer chosen for BPA has the sequence 5′-CCGG TGGG TGGT CAGG TGGG ATAG CGTT CCGC GTAT GGCC CAGC GCAT CACG GGTT CGCA CCA-3′ and for this aptamer named aptamer #3, K_d for BPA, 6 F, BPB, and BP are 8.3 nM, 208 mM, 139 mM, and 139 mM, respectively.[90] The specified aptamer was used in at least 90% of BPA aptamer studies reported in this review (Table 2).

BPA biosensor methods have evolved into much more sensitive techniques with relatively low cost, high accuracy, and improved user compatibility. Aptamers were used to provide selectivity in these sensors. Sensor platforms using aptamers can be based on electrochemical, fluorescence, luminescence, colorimetry, Raman scattering, surface plasmon resonance, and other techniques (Table 3). These techniques have been successfully applied in real samples or matrices by sample addition. Sensitivity, operating range, and actual condition performances are listed to evaluate the quality of analytical results of these sensors from a glance of general perspective. Especially with the use of the same aptamer in many sensor platforms, a convenient comparison has emerged. In recent years, two BPA-focused reviews were published focusing on the BPA detection techniques for foodstuffs and summarizing different detection strategies.[143,144] Furthermore, a more specific review article recently presented a detailed update on the development of polymer and metal-based graphene electrochemical sensors.[145] On the other hand, this comprehensive review summarizes the main strategies of aptamer-based BPA detection in the last decade as well as provides a critical discussion on analytical parameters and a statistical evaluation. Due to many studies in the literature, some studies may not be mentioned in this comprehensive review article. However, we believe that the studies mentioned in this review could provide information for a general evaluation.

Electrochemical sensors

Electrochemical-based sensors, as well as for the detection of other analytes, have been the most studied BPA sensor platform for their ease of use, sensitivity, and versatility. In this section, electrochemical-based aptasensors used in BPA detection are discussed.

Anodized aluminum oxide (AAO) based capacitive sensor was reported in one of the first studies of electrochemical-based BPA aptasensors. In this sensor, after the deposition of Au film as an electrode on the AAO membrane, Au nanowires in the AAO nanopores were used as the other electrode. A change in the aptamer's dielectric properties or capacitance was observed because of BPA binding with the aptamer attached to both electrodes. In this way, 43 nM of BPA LOD and 0.1–100 nM detection range were achieved quite successfully.[116]

A sensor platform based on the competitive binding of BPA to the aptamer has also been proposed. In this study using a gold electrode, a signal was obtained when the other methylene blue (MB) labeled ssDNA pre-attached to the aptamer was released in the presence of BPA. It has been reported that this sensor operating in the range of 0.44 pM–4.4 nM gives a LOD of 1.24 pM and provides good recovery in different water samples.[117] In another simple

Table 2. BPA aptamers that are reported in the literature (modeling of aptamers was done with DNAFold.[91]

Sequence (5' to 3')	DNAFold model	Applied by
CCGGTGGGTG[10] GTCAGGTGGG[20] ATAGCGTTCC[30] GCGTATGGCC[40] CAGCGCATCA[50] CGGGTTCGCA[60] CCA	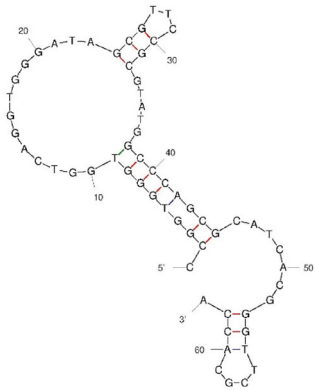	[92] [93] [94] [95] [96] [97] [98] [99] [100] [101] [102] [103] [104] [105] [106] [107] [108] [97] [109]
CCGGTGGGTG GTCAGGTGGG ATAGCGTTCC GCGTATGGCC CAGCGCATCA CGGGTTCGCA CC	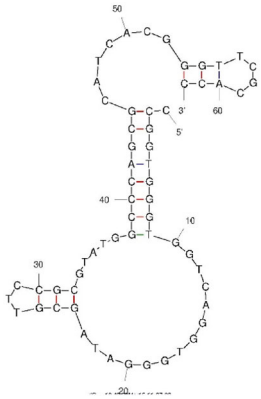	[110]
TTTTTTTTTT GGATAGCGGG TTCC	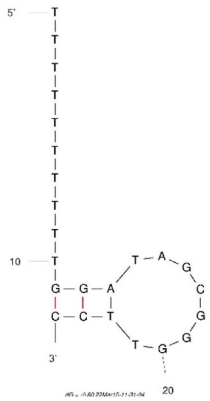	[111] [64] [7]
GGGCCGTTCG AACACGAGCA TGCCGGTGGG TGGTCAGGTG GGATAGCGTT CCGCGTATGG CCCAGCGCAT CACGGGTTCG CACCAGGACA GTACTCAGGT CATCCTAG	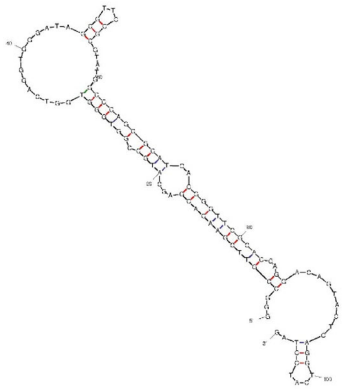	[102]

(*continued*)

Table 2. Continued.

Sequence (5' to 3')	DNAFold model	Applied by
CCGCCGTTGG TGTGGTGGGC CTAGGGCCGG CGGCGCACAG CTGTTATAGA CGTCTCCAGC	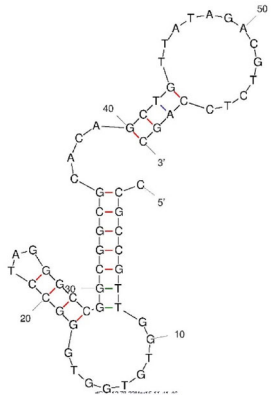	[112]
GGGCCGTTCG AACACGAGCA TGCCGGTGGG TGGTCAGGTG GGATAGCGTT CCGCGTATGG CCCAGCGCAT CACGGGTTCG CACCAGGACA GTACTCAGGT CATCC	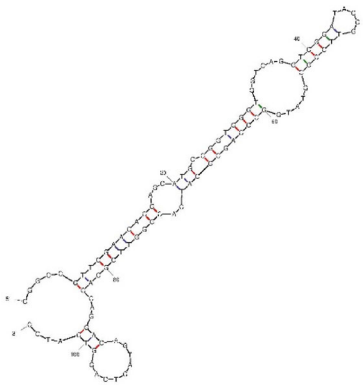	[113]

Folding conditions are 25 °C, 100 mM Na^{+} and 100 mM Mg^{2+}. The numbers given as superscripts represented the number of bases from the specified termini).

and sensitive (5 nM LOD) electrochemical sensor platform, the signal was obtained on the glassy carbon electrode (GCE) using gold nanoparticles (AuNPs) dotted graphene nanocomposite film. In this study, using ferricyanide mediator, cyclic voltammetry (CV) and differential pulse voltammetry (DPV), a sensor operating in the range of 10 nM–10 μM, which can respond to milk and milk powder samples, was developed.[108] An aptasensor using a GCE electrode and DPV achieved a low LOD level of 56 pM using nanoporous gold film. This nanoporous film obtained by dealloying Ag from Au/Ag alloy using concentrated nitric acid was used in the serum sample with good recovery (98.9–102.3%) for BPA detection. The operating range of this sensor was 1–100 nM.[107]

A highly sensitive BPA sensor, on the other hand, was based on the AC electrokinetics (ACEK) capacitive sensing principle. It utilizes AC signal over microelectrodes to generate local fluid motion which facilitates particle movement and enrichment. In this method, the binding of BPA to the aptamer changed the capacitance of the fluid/electrode interface. This sensor, which measures in the range of 10 fM–10 pM, was used to detect BPA from serum samples.[106] In another study using the AC signal, an excellent LOD of 73.2 aM was reported in porous interdigitated electrodes (flexible polyimide sheets) and an aptamer-based sensor. Cheng *et al.* reported a very successful recovery (83.6–100.7%) in surface water samples in this study while reporting a working range (0.1 fM–1 pM) proportional to the sensitivity of the sensor.[122] Using the printed circuit board and GCE platform, the same group achieved 152 aM LOD. This sensor was used to detect BPA in canned food, but the recovery was slightly lower.[74]

Alternative signal amplification methods have also been frequently studied. Ferrocene (Fc)-labeled BPA-binding aptamer probe and MB-labeled complementary probe were used on a sensor platform working with the sum of three different signals. During binding, MB-labeled ssDNA moved away from the surface and produced a signal, while Fc-labeled aptamer provided a signal with conformational change. In addition, 0.19 pM LOD was obtained with a gold electrode by combining the signal obtained from BPA. This sensor, which operates in a relatively narrow detection range (1–100 pM), has been successfully used in tap-water samples.[118] The same group also obtained a dual signal by using avidin-horseradish peroxidase (HRP)-AuNP enzyme-based assay together with redox target BPA. Upon the specific interaction between BPA and its aptamer, the aptamer and complementary DNA duplex was dissociated. Meanwhile, in addition to the received signal, "signal-off" behavior was obtained in the signal catalyzed due to the avidin complex.[120] A low LOD of 0.41 pM was obtained from this sensor, which was also tested in real samples in the 1 pM–1 nM range.

An electrochemical aptasensor was designed for the detection of BPA using aptamer conjugated with MB and gold-coated multi-walled carbon nanotubes (MWCNTs) to

Table 3. Aptamer based BPA biosensors.

Method	Year	Approach /Strategy	LOD	Range	Recovery %	Real Samples	Ref.
Colorimetric	2015	Cysteamine modified gold nanoparticles (AuNPs), aptamer	0.48 nM	153–613 nM	91.0–106.0	Tap water	[114]
Colorimetric	2016	Cationic polymer-induced aggregation of AuNPs, aptamer	1.50 nM	1.50–500 nM	100.9–112.7	Tap and river water	[92]
DNA amplification	2018	Aptamer coated well and real-time quantitative PCR (RT-qPCR)	0.7 nM	1–500 nM	96.8–104.0	Water	[115]
Electrochemical (1)	2011	AAO, aptamer	43 nM	0.1–100 nM	NR	NR	[116]
Electrochemical (2)	2013	Gold electrode, aptamer	1.24 pM	0.44 pM–4.4 nM	94.0–103.0	Water	[117]
Electrochemical (3)	2014	AuNPs dotted graphene nanocomposite film modified GCE, aptamer	5 nM	10 nM–10 μM	90.0–116.0	Milk and milk powder	[108]
Electrochemical (4)	2015	Nanoporous gold film, GCE, aptamer	56 pM	1–100 nM	98.9–102.3	Serum	[107]
Electrochemical (5)	2015	AC signal, microelectrodes, capacitive, aptamer	10 fM	10 fM–10 pM	NR	Serum	[106]
Electrochemical (6)	2016	Fc-modified aptamer, gold electrode	0.19 pM	1–100 pM	96.0–104.0	Tap water	[118]
Electrochemical (7)	2016	Poly(pyrrole-Nitrilotriacetic Acid)–$[Ru^{III}(NH_3)_6]^{3+}$ complex, GCE, aptamer	10 pM	10 fM–1 μM	NR	NR	[119]
Electrochemical (8)	2016	Platinum nanoparticles (PtNPs), acid-oxidized CNTs (CNTs–COOH) functionalized with PEI, GCE, aptamer	230 pM	50–400 nM	93.1–108.5	Water	[99]
Electrochemical (9)	2016	Horseradish peroxidase-catalyzed, AuNPs, GCE, aptamer	0.41 pM	1 pM–1 nM	95.0–105.0	Tap water	[120]
Electrochemical (10)	2016	AuNPs, PB functionalized CNTs, aptamer	0.045 pM	0.1 pM–10 nM	95.5–103.4	Water	[121]
Electrochemical (11)	2016	Porous interdigitated electrodes (flexible polyimide sheets), aptamer	73.17 aM	0.1 fM–1 pM	83.6–100.7	Surface waters	[122]
Electrochemical (12)	2017	Printed circuit board and GCE platform, aptamer	152 aM	1 fM–10 pM	75.1– 106.1	Canned foods	[74]
Electrochemical (13)	2017	AuNPs coated boron-doped diamond (BDD), aptamer	7.2 fM	10 fM–1 nM	92.0–108.0	Milk	[101]
Electrochemical (14)	2017	Au-PtNPs, GCE, CNTs, aptamer	0.035 pM	0.1–700 pM	94.5–103.6	Tap water	[97]
Electrochemical (15)	2017	MWCNTs, AuNPs, gold electrode, aptamer	0.05 nM	0.1–10 nM	96.0–106.0	Mineral water, orange juice and milk	[123]
Electrochemical (16)	2018	AuNPs, MWCNTs, and thiol-functionalized magnetic Fe_3O_4 nanoparticles, aptamer	0.03 nM	0.1–8 nM	97.5–120.5	Water, milk and juice	[124]
Electrochemical (17)	2018	AuNPs, GCE, aptamer	44 fM	0.11–8.76 pM	95.0–103.0	Red wine	[125]
Electrochemical (18)	2018	Integrated microfluidics on gold electrode, aptamer labeled with Fc	0.2 pM	5 pM–1 nM	95.0–108.0	Saliva and plasma	[109]
Electrochemical (19)	2018	Aptamer extension reaction triggered by terminal deoxynucleotidyl transferase, Fc transfer blocking	15 pM	0.08–15 nM	88.6–97.3	Tap water and grape juice	[98]
Electrochemical (20)	2019	MWCNTs, SiO_2@Au particles, GCE, aptamer	10 pM	0.1–100 nM	96.0–108.0	Milk, orange juice	[36])
Electrochemical (21)	2019	MWCNTs, Au coated carbon tape and polyethylene terephthalate electrode, aptamer labeled with MB	8 fM	10 fM–1 nM	88.0–106.2	Bottles, water, milk	[126]
Electrochemical (22)	2019	Au electrode, single-stranded DNA (ss-DNA), propargyl-2-bromoisobutyrate, Fc methyl methacrylate, aptamer	59 aM	10 fM–100 nM	95.2–98.4	Water	[127]
Electrochemical (23)	2019	ssDNA-MB complex, and aptamer	1.75 pM	4.4 pM–440 nM	88.7–125	Tap water, bottle and toy	[75]
Electrochemical (24)	2019	Mixture of carboxylated MWCNTa and chitosan, aptamer	0.38 nM	0.2–2 nM	84.5–88.2	Serum	[128]
Electrochemical (25)	2019	Au-coated MWCNTs, ssDNA-dye complex, aptamer	8 fM	10 fM–1 nM	88.0–106.2	Water, milk, bottle	[126]
Electrochemical (26)	2020	Screen-printed carbon electrode (SPCE), Au NPs, aptamer	0.113 pM	1 pM–10 nM	93.8-97.3	Serum	[129]
Electrochemical (27)	2021	AuNPs, $CuFe_2O_4$ functionalized NPs, MWCNTs, GCE, aptamer	25 pM	0.05–9 nM	98.9–110.5	Water, milk, juice	[130]
Electrochemical (28)	2022	Target-induced chain release, dendritic AuNPs, aptamer functionalized with MB	0.98 nM	1.0–500 nM	93.8–104.9	Tap and mineral water, milk	[131]
Electrochemiluminescent	2018	Carboxylated graphitic carbon nitride (C-g-C_3N_4), aptamer	30 fM	0.1 pM–1 nM	97.1–104.2	Tap water, orange juice	[132]
Field-effect transistor	2016	Aptamer-modified multichannel carbon nanofibers (MCNFs)	1 fM	1 fM–10 pM	NR	NR	[100]
Fluorescence	2013	Aptamer tagged with fluorescein amidite and black hole quencher (BHQ-1) at both termini	0.044 pM	0.44 pM–43.8 nM	NR	Urine, water	[133]
Fluorescence	2015	GO, aptamer	0.21 nM	0.43–43 nM	96.0–104.5	Water	[111]
Fluorescence	2017	Mesoporous silica nanoparticles loaded with rhodamine B and capped with a BPA aptamer	3.5 μM	4–100 μM	NR	Water	[134]
Fluorescence	2017	Magnetic bead, quantum dots, aptamer	0.74 pM	4.4 pM–43.8 nM	NR	NR	[86]
Fluorescence	2017	N-methylmesoporphyrin IX, Mo_2C nanotubes, aptamer	2 nM	2–20 nM	NR	Water	[135]

(*continued*)

Table 3. Continued.

Method	Year	Approach /Strategy	LOD	Range	Recovery %	Real Samples	Ref.
HPLC/magnetic seperation	2020	Silica-coated Fe_3O_4 magnetic microspheres, aptamer	0.22 nM	0.44–438 nM	78.0–113.0	Milk	[136]
HPLC/magnetic seperation	2018	Fe_3O_4@SiO_2 magnetic nanoparticles, aptamer	4.38 nM	0.022–44 μM	90.8 ± 7.3%	Serum, urine	[137]
Optical spectroscopy	2014	Plasmonic chirality, aptamer	0.35 nM	0.88–21.9 nM	93.0–98.4	Tap water	[138]
Optical spectroscopy	2019	Plasmonic, localized plasmon resonance, Au micro-antenna, aptamer	0.33 fM	1 fM–10 nM	NR	NR	[7]
Photoelectrochemical	2018	TiO_2 nanoparticles embedded in borocarbonitride nanosheets, aptamer	0.03 fM	0.1 fM–5 nM	88.0–104.2	Drinking water	[139]
Photoelectrocehmical	2022	MoS_2/Ni-Fe layered double hydroxide heterostructure and aptamer	22.7 fM	0.22–43.8 pM	98.60–100.53	River water	[140]
SERS	2014	MBA raman reporter, AuNPs, polyethyele glycol mixed self assembled monolayers, aptamer	3 nM	∼3–300 nM	NR	NR	[141]
SERS	2018	Chitosan encapsulated -MBA coated Au@AgNP, aptamer	12.3 pM	0.44–4.38 nM	91.0–103.5	Bottled water and milk	[142]

achieve dual signal amplification.[126] Competitive binding of BPA and MB to the aptamer causes a conformational change of MB-aptamer and release of MB and a decrease in signal. BPA detection in the range of 10 fM to 1 nM was performed under optimal conditions and a LOD of 8 fM was reported. In real samples, 88.0–106.2% recovery was obtained.

In another electrochemical sensor with sub-nanomolar LOD performance, platinum nanoparticles and acid oxidized CNTs modification and polyethyleneimine (PEI) were used on GCE. A LOD level of 230 pM was obtained with <10% RSD in real water samples.[99] In a study using Prussian blue (PB) functionalized CNTs redox tag, Azadbakht et al. reported a simple, rapid, and sensitive method providing 0.045 pM LOD in the 0.1 pM–10 nM range. When BPA was added, an impedimetric signal was obtained with the formation of the BPA/aptamer complex.[121]

Efforts to increase the sensitivity of the electrochemical sensor with the use of nanomaterials have been published quite frequently. Aptasensors used in various real samples in studies reporting subpicomolar (∼fM) LOD are presented. AuNPs coated boron-doped diamond aptasensor delivered a 7.2 fM LOD in the 10 fM–1 nM range.[101] A 35 fM LOD was obtained in a GCE electrochemical sensor based on Au-PtNPs and CNTs.[97] In another GCE-based approach, Shi et al. reported 44 fM LOD using AuNPs, and in this study 95.0–103.0% recovery was obtained in red wine.[125] Electrochemical sensors were also developed, this time providing subnanomolar LOD, using the advantages of nanomaterials. Using MWCNTs and AuNPs on the gold electrode, Deminiat et al. proposed a sensor platform that provides 50 pM LOD and operates in the 0.1–10 nM range. It was successfully used to detect BPA with 96.0–106.0% recovery in mineral water, orange juice, and milk samples.[123] Using a similar modification, Baghayeri et al. proposed a sensor that detects BPA with slightly excess RSD% in real samples of water, milk, and juice, this time using the magnetic Fe_3O_4 nanoparticles. This platform provided a LOD of 30 pM in the range of 0.1–8 nM.[124] In addition, core-shell nanoparticles have also yielded successful results. In a study using MWCNTs, SiO_2@Au particles, Razavipanah et al. reported 10 pM LOD, and this sensor was used to detect spiked BPA from milk and orange juice samples with <10%RSD.[36] In a study using AuNPs, $CuFe_2O_4$, and MWCNTs, 25 pM LOD was obtained.[130] In this study, where real samples of water, milk, and juice were used, the recovery obtained from the sensor, which responded in the range of 0.05–9 nM, was between 98.9–110.5%. An electrochemical aptasensor platform based on atom transfer radical polymerization (eATRP) signal amplification revealed a low LOD of 59 aM. The high recovery of 95.23–98.40% obtained in real samples demonstrated the analytical performance of the sensor. It is seen that the proposed innovative signal amplification approach is successful in this method, where signals are obtained from Fc with eATRP click-chemistry.[127]

In a sensor platform using integrated microfluidics, the Fc-labeled aptamer increased the signal in the presence of BPA as the Fc label approached the surface (Figure 1(a)). A 0.2 pM LOD was reported in the 5 pM–1 nM operating range, demonstrating the advantage provided by such switched sensors. This aptasensor provides a precise platform for simple, selective, and more importantly rapid detection of BPA. In addition, 95.0–108.0% recovery was obtained in saliva and plasma samples.[109] The advantage of using labeled aptamer was also demonstrated by Yu. In their study using MB as the label, the authors reported a very low LOD of 1.75 pM and a range of 4.4 pM–440 nM in terms of analytical performance using disposable gold film modified polyethylene terephthalate electrode (Au/PET electrode). However, the recovery deviation of the proposed sensor was as high as 25% RSD in tap water, bottle, and toy real samples.[75] Nazari et al. obtained 84.5–88.2% recovery on the surface of a mixture of carboxylated MWCNT and chitosan with an Fc-labeled aptamer applied in serum samples. In terms of analytical performance, LOD value of 380 pM was quite successful.[128] The difficulty of working with serum samples can be understood from the negative biased recovery values (despite the use of chitosan). Abnous et al. suggested nontarget-induced bridge assembly and aptamer extension reaction triggered by terminal deoxynucleotidyl transferase (TdT) and Fc transfer blocking as a different approach to signal enhancement (Figure 1(b)). This platform has shown high sensitivity due to the formation of a physical barrier on the surface of the electrode in the absence of a target, with a LOD of 15 pM over the linear range of 0.08–15 nM. In addition, 88.6–97.3% recovery was obtained in real samples of tap water and grape juice.[98]

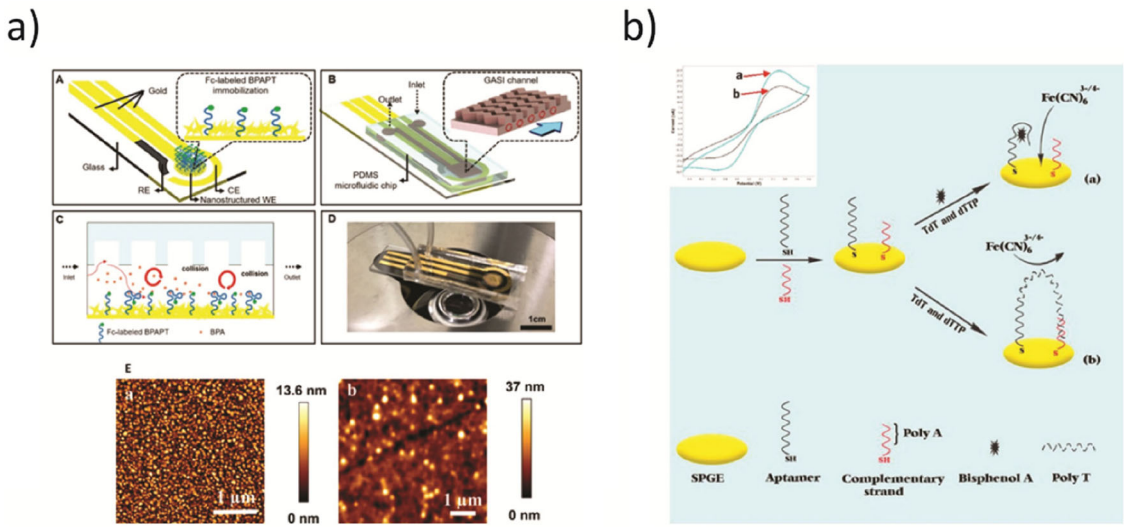

Figure 1. Schematic representations of **a)** the different steps of fabrication of the MEA for detection of BPA (A) A schematic design for immobilization of BPA-aptamer onto the surface of the nano-structured electrode, (B) MEA and GASI channel, (C) Schematic of interaction between BPA and BPAPT inside the microchannel, (D) A photograph of MEA, (E) AFM images of Bare (a) and (b) aptamer-modified NSGE.[109] **b)** the electrochemical aptasensor for BPA detection based on a non-target-induced extension of aptamer length triggered by TdT.[98]

Another approach in tagged aptasensor platforms was to amplify the sensor signal using the conjugated ssDNA tag complex. By combining the ssDNA–MB complex with Au-coated MWCNTs (Au/MWCNTs), a quite low detection limit of 8 fM was obtained in a detection range of 10 fM–1 nM. In addition, 88.0–106.2% recovery was obtained in real samples using this sensor, in bottles, water, and milk samples with an inexpensive platform..[126]

A similar approach with a much lower (59 aM) detection limit was obtained using Fc, ss-DNA, propargyl-2-bromoisobutyrate, and aptamer. The sensor operating over a wide range compared to the detection limit (10 fM–100 nM) had a recovery rate of 95.2–98.4% from water samples.[127] In another study, Li et al. reported a sensor operating in the range of 10 fM to 1 nM with a LOD of 8 fM using Au-coated MWCNTs and ssDNA-dye complex. The real sample (water, milk, and bottle) performance of this sensor was also quite successful.[126]

In a recent study, an alternative route was followed by using target-induced chain release, dendritic AuNPs, and aptamer functionalized with MB. In this study, the MB signal increased when the labeled double-strand was opened when BPA was added, followed by the folding of the aptamer into the G-quadruplex structure by BPA. Reported to operate in the 1.0–500 nM range, this sensor provided a detection limit of 980 pM. BPA in real samples of tap and mineral water and milk was detected with <6% RSD.[131]

By performing the principal component analysis (PCA) of the electrochemical sensors discussed in this review article, the results of analytical performance indicators such as detection limit (log(LOD), nM), operating range (log(upper limit-lower limit), nM), and recovery (maximum deviation as a percentage) were compared. Figure 2 shows the biplot giving scores and loading. It is seen that electrochemical studies do not form separate groups in terms of LOD, range, and RSD%. On the other hand, in terms of LOD and range vectors, the study, which reported a LOD value of 59 aM, stands out.[127] In addition, studies that are out of the cluster in terms of RSD% and result in high RSD% are studies that detect BPA in matrices other than water (such as plastic bottles, milk, and serum). In addition, in the classification performed by considering different strategies, methods that use electrode modification, signal enhancement with nanoparticle addition, use of aptamer-conjugated labels, aptamer binding, and labeled ssDNA release strategies individually or together were also subjected to PCA analysis. However, it has been observed that any approach does not differentiate in terms of analytical performance.

The contour plot shows that only 4 studies differ from the group in terms of LOD, range, and RSD%. A high range is not important on its own, but its presence in combination with a low LOD indicates that the analytical performance of the sensor is successful. Among the electrochemical aptasensors examined in this study, the reports numbered 22, 10, 9, 6, 14, and 17 given in Table 3 seem to be successful in terms of analytical performance compared to other studies. In the article reported by Li et al., after the detection of BPA by the recognition element, the amplification provided by Cu catalyzed electrochemically mediated atom transfer radical polymerization (eATRP) provided high analytical performance in terms of both detection limit and detection range.[127] A very wide detection range was also obtained because of the amplification performed after the binding of the analyte. Finally, the combination of a specific recognition element such as the aptamer and the electrochemical method provided usability with real samples. However, it should not be forgotten that the use of only water samples in the study also contributes to this real sample performance. In addition, the use of the truncated version of the previously reported BPA-specific aptamer, the short aptamer, in this study may also contribute to performance.

On the other hand, in two studies that differed in terms of analytical performance indicators (shown in Table 3 as 10 and 6), it was observed that the redox tag was integrated

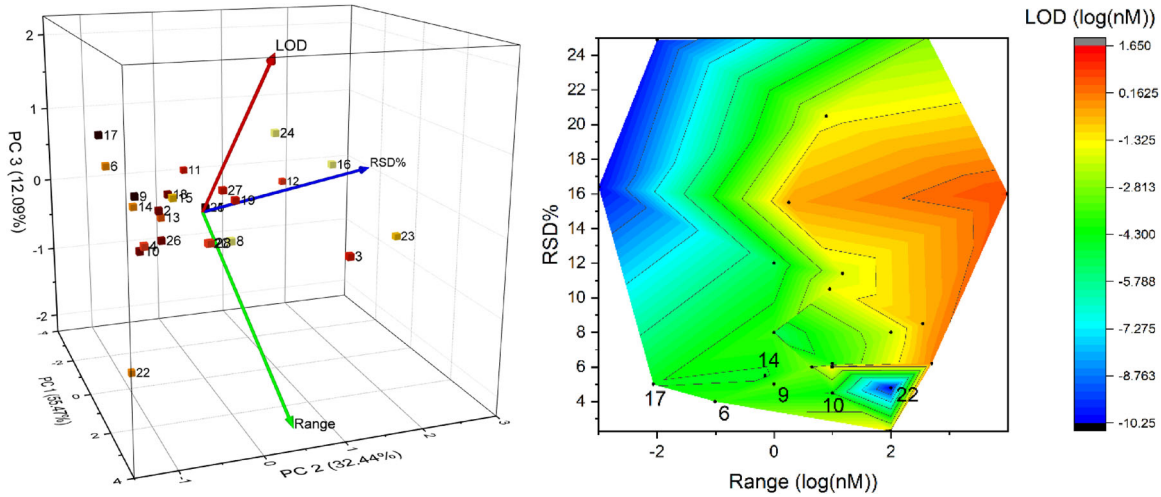

Figure 2. Analytical performance grouping of electrochemical BPA sensors discussed in this review article (A) PCA, (B) contour plot of analytical performance indicators.

into the electrode after different nanomaterial modifications. Azadbakht et al. achieved high analytical performance because of in situ formation of PB and integration of AuNPs and oxide CNTs into the decorated electrode. By adding BPA as the target and upon the formation of the BPA/aptamer complex on the electrode surface, the electron transfer characteristics of PB as the electrochemical indicator were retarded.[121] While Liu et al. applied similar nanomaterial modification (this time Au-Pt nanoparticles), this time he modified the aptamer with acriflavine (ACF) as a redox probe, increasing the analytical performance. In this sensor, BPA caused the aptamer to be folded and the formation of BPA-aptamer complexes at the sensing interface hindered the interfacial electron transfer of the probe, resulting in the decrease of the electrochemical signal.[118] Another study showing the advantage of labeling the aptamer probe directly with the redox probe was reported by Beiranvand. In this study, MB-tagged complementary oligonucleotide and aptamer were used. In this sensor, BPA makes the dissociation of MB-labeled complementary DNA from the immobilization site. As a result, the MB tags are released from the electrode surface and BPA is close to the electrode surface, leading to a decrease in the oxidation peak current of MB and an increase in that of BPA.[97] It can be said that the integration of this redox probe, which is seen to provide an advantage compared to other studies in terms of analytical performance indicators, directly to the electrode, aptamer, or a secondary complementary oligonucleotide connected to it, has increased the analytical performance.

Two other studies, which had better analytical indicators compared to other studies on electrochemical sensor platforms, applied different amplification strategies. In one of these studies, the detection signal was enzymatically amplified with the avidin-HRP-AuNP probe.[120] The working principle is as follows: upon the specific interaction between BPA and its aptamer, the aptamer/complementary DNA duplex is separated. This separation then causes an increase in BPA signal and a decrease in avidin-HRP-AuNP catalyzed signal. Shi et al. used the Exo III-induced signal recycling amplification strategy. According to this strategy (Figure 3 capture DNA (cDNA) was immobilized on the porous Au electrode. In the presence of immobilized aptamer BPA on the magnetic bead, the message DNA (mDNA) strand was released. After hybridization of mDNA and cDNA, ExoIII and cDNA were separated from each other. Since the amount of cDNA is proportional to BPA, another sequence (hDNA) and reporter DNA (rDNA) immobilized on AuNP was captured using the MB tag. The amplified signal obtained after this treatment demonstrated an analytical performance providing a detection limit of 44 fM in the 0.11–8.76 pM operating range.[125]

Overall, the electrochemical aptasensors reported for BPA appear to receive signals using different strategies. It is possible to group these strategies as electrode modification, using a label on the aptamer or the nanomaterial to which it is attached, and using enzymatic or alternative amplification methods. As expected, different electrode modifications and the use of nanomaterials improve analytical performance measures in BPA detection. However, a strategy of attaching a label to one end of the aptamer or the nanomaterial to which the aptamer is attached has also provided very high analytical performances. While some of these studies provide a very low detection limit and wide detection range, it is also seen that the recovery % performances are high in the real sample. Moreover, we also found that alternative detection methods (multi-step amplification methods) have quite good analytical performance indicators in terms of detection limit and range. On the other hand, all electrochemical aptasensor approaches discussed in this review article have sufficient analytical performance to measure allowable residue and maximum migration limits for BPA.

Fluorescence-based sensors

Fluorescence-based sensors are another platform developed for BPA detection and are highly preferred by researchers. Fluorescence-based sensors, like other sensor platforms, have their advantages and disadvantages. Herein, from the perspective we set out in this review article, we compared

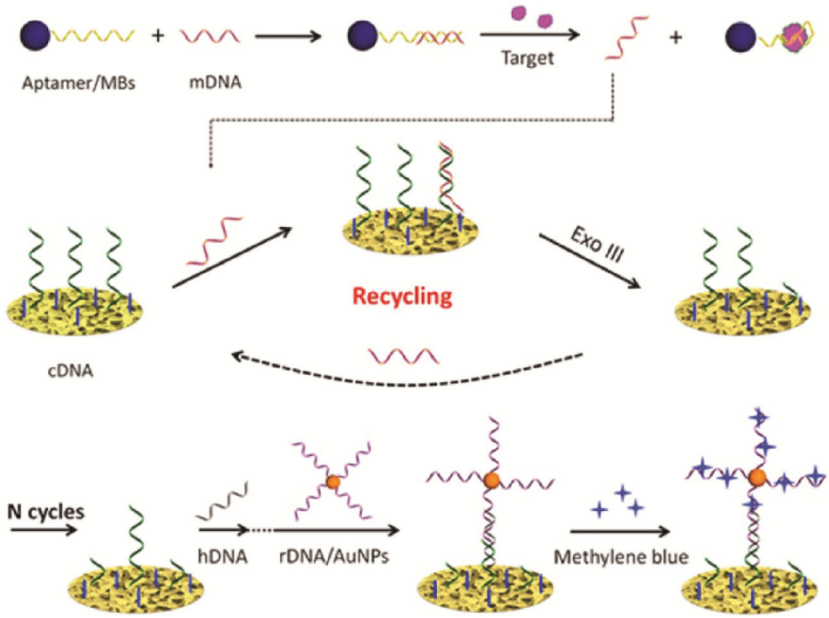

Figure 3. Schematic representations of the amplification strategy for sensitive detection of BPA.[125]

aptasensors by evaluating strategies to increase analytical performance indicators.

In the first reports of fluorescence-based aptasensors, we come across a study in which the aptamer was tagged from both termini with a fluorescein tag and a quencher. The unique 3 D structure of the aptamer in the presence of BPA caused a decrease in the fluorescent signal, allowing a detection limit as low as 44 fM to be reached. This low LOD provided by the amidite and black hole quencher pair provided a very high analytical performance with a very wide working range (0.44 pM–43.8 nM). Although the recovery from real samples of urine and water was not directly reported, it was stated that real sample application was carried out successfully.[133] In another study in which the Förster resonance energy transfer (FRET) strategy was applied, GO and fluorescein amidite (FAM)-labeled aptamer was used as fluorescence quenching agents. A detection limit of 210 pM was obtained because of the principle of observing the fluorescent signal with protection thanks to the conformation switch formed in the presence of BPA. 96.0–104.5% recovery was obtained in real water samples of this sensor.[111] Ribes et al. loaded rhodamine B onto mesoporous silica nanoparticles and then capped them with a BPA aptamer. The detection limit of this sensor, which can detect in the range of 4–100 µM BPA, was 3.5 µM.[134]

It is a known approach to alter the affinity of a previously selected aptamer sequence by truncation or mutation. Using this approach, a 0.74 pM LOD was obtained with the aptamer conjugated on magnetic bead-quantum dots.[86] A 39 pM LOD was also obtained with an aptasensor using SYBR Green I and AuNPs.[146] The analytical performance of the approach presented here was quite good and included a basic mechanism as seen in Figure 4.

Linearity in the range of 2–20 nM with a detection limit of 2 nM for detecting BPA was obtained using Mo_2C nanotubes and N-methylmesoporphyrin IX dye in a label-free approach. In this study, a signal was obtained because of G-quadruplex between G-rich splits GGGT of the anti-BPA aptamer and G-rich sequence (TGGGTGGG TGGGT) at the 5′-terminal of the Help-DNA formation.[135] The authors also reported that the background signal was eliminated using Mo_2C nanotubes.

Overall, the analytical performance of the fluorescent-based sensors discussed in this article appears to be lower than the electrochemical sensors. While the average LOD values for electrochemical sensors (log(LOD), nM) are −3.37, it is seen that only two fluorescent-based sensors can reach this average value.[86,133] Moreover, there is not enough data about working on real samples in fluorescent-based aptasensors. In addition, nearly all the fluorescent-based sensors on the list have been found to provide adequate analytical performance suitable for detecting residual BPA levels.

Colorimetric and plasmonic sensors

Another approach used in BPA detection is the use of colorimetric-based sensor platforms. In this section, we have not only considered colorimetric sensors, but also plasmonic sensors. Generally, in the colorimetric approach, AuNPs, which benefit from plasmonic properties, are utilized due to both the ease of modification (in other words, the ease of conjugation of the aptamer to the nanoparticle) and the tunable colorimetric properties. Therefore, two aptasensors discussed in our review article use AuNP. In one study, AuNPs that are positively charged due to the modification with cysteamine which is cationic at near-neutral pH values were used. The color change obtained by removing the blue shift caused by the addition of the aptamer due to the selective interaction between BPA and the aptamer was obtained as a signal. This sensor, which can operate in the range of 153–613 nM, provided a very suitable detection limit of 0.48 nM. In the experiments performed with tap water,

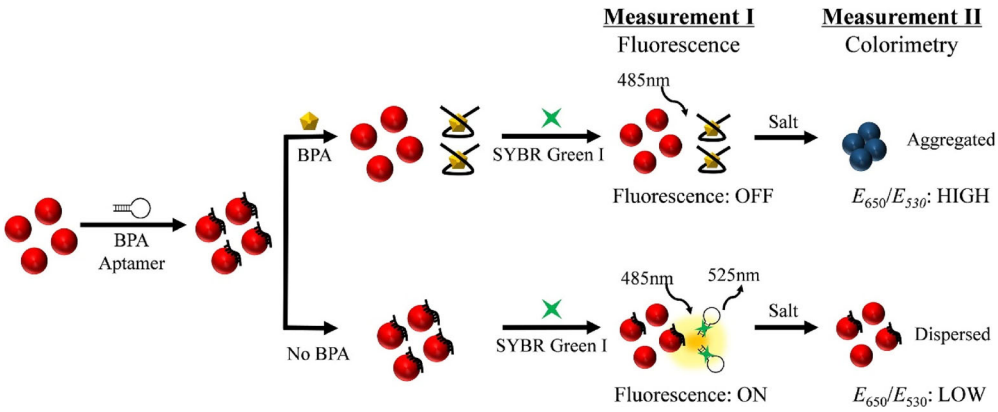

Figure 4. Schematic of the detection principle using aptamer-associated gold nanosensors with SYBR Green-I (SG-I) for the sensitive detection of BPA. The presence of BPA modulates two independent signals without cross-reactivity, leading to a decrease in fluorescence emission and a higher extinction ratio (E650/E530) because of salt-induced aggregation in the gold nanoparticle (AuNP) solution. Compared with classical aptamer/AuNP colorimetry at a high salt concentration, this fluorescence-combined colorimetric approach can detect BPA with enhanced sensitivity and selectivity.[146]

91.0–106.0% recovery was obtained.[114] In the other colorimetric approach, cationic polymer-induced aggregation of AuNPs was used. In this sensor platform, which provides 100.9–112.7% recovery in real samples of tap and river water, measurements were made in the range of 1.50–500 nM BPA. The detection limit of this aptasensor platform was 1.50 nM.[92]

In the surface-enhanced Raman spectroscopy technique, in which plasmonic structures are used, successful analytical performance results were reported with the use of aptamer as a diagnostic element. Marks et al. reported a SERS platform operating in the ~3–300 nM range and providing a detection limit of 3 nM using 4-mercaptobenzoic acid (MBA) Raman reporter, AuNPs, polyethylene glycol mixed self-assembled monolayers, and BPA specific aptamer.[141] In another study where the detection limit was lowered, MBA was encapsulated with chitosan this time and Au@Ag core-shell nanoparticle was used as the plasmonic structure. This sensor provided a detection limit of 12.3 pM, providing 91.0–103.5% recovery in bottled water and milk real samples.[142]

Another plasmonic sensor, which provides a very high analytical performance, used combined localized plasmon resonance signals. Allsop et al. developed a plasmonic biosensor in which BPA is detected with a detection limit of 330 ± 70aM and the sensitivity is 0.15 ± 0.01 nm wavelength shift/fM BPA.[7] This low detection limit achieved by this system, which uses immobilized aptamer and signal-coupled localized surface plasmons on a series of gold nano-antennas, is very promising. The performance of this sensor, which offers a successful sensitivity and detection limit in the detection of low molecular mass analytes such as BPA, was evaluated only in buffer (Figure 5).

Other methods using BPA aptamers

Different sensor platforms have also been proposed for BPA detection using BPA-specific aptamer. One of these platforms is based on real-time quantitative PCR (RT-qPCR). After coating the BPA aptamer in the well, BPA detection was achieved, and then the signal was increased by amplification with PCR. A detection limit of 0.7 nM was achieved in this DNA amplification method. While 96.8–104.0% recovery was obtained in various water samples, the operating range of the sensor platform was reported as 1–500 nM.[115]

In two similar studies as a detection approach, aptamer was used for preconcentration for HPLC. Detection of BPA after its isolation by magnetic separation increased the analytical performance of the sensor. In both studies, aptamer immobilized on the carrier obtained by SiO_2 coating of magnetic Fe_3O_4 nanoparticles was used. In the first study in which BPA was detected from real samples of serum and urine, 90.8 ± 7.3% recovery was achieved, and the detection limit was reported to be 4.38 nM. As an advantage of chromatographic techniques such as HPLC, the working range was from 22 nM to 44 µM.[137] Then the analytical performance (in terms of detection limit) was further improved. LOD value of 220 pM was reported with the HPLC/magnetic separation platform, which can detect in the range of 0.44–438 nM. Again, this platform, where real sample tests were carried out in a complex environment, provided 78.0–113.0% recovery from milk.[136]

Although they are similar in principle to electrochemical sensor platforms, other BPA aptasensor platforms that we consider appropriate to consider in the other methods section are electrochemiluminescent and photoelectrochemical platforms. Cao et al. reported a novel electrochemiluminescence (ELC) sensing platform using carboxylated graphitic carbon nitride (C-g-C_3N_4) and NH_2-aptamer. Interaction of aptamer because of interaction with BPA caused a decrease in ELC signal. With this signal change, a BPA sensor operating in the range of 0.1 pM–1 nM and providing a detection limit as low as 30 fM has been reported. Real sample experiments were carried out with the detection of BPA in tap water and orange juice, and 97.1–104.2% recovery was obtained.[132] Two different photoelectrochemical (PEC) aptasensor platforms also provided highly successful analytical results. In the first report, a very wide detection range (0.1 fM–5 nM) was obtained using TiO_2 nanoparticles embedded in borocarbonitride nanosheets and aptamer. The detection limit of this sensor platform was 0.03 fM and was

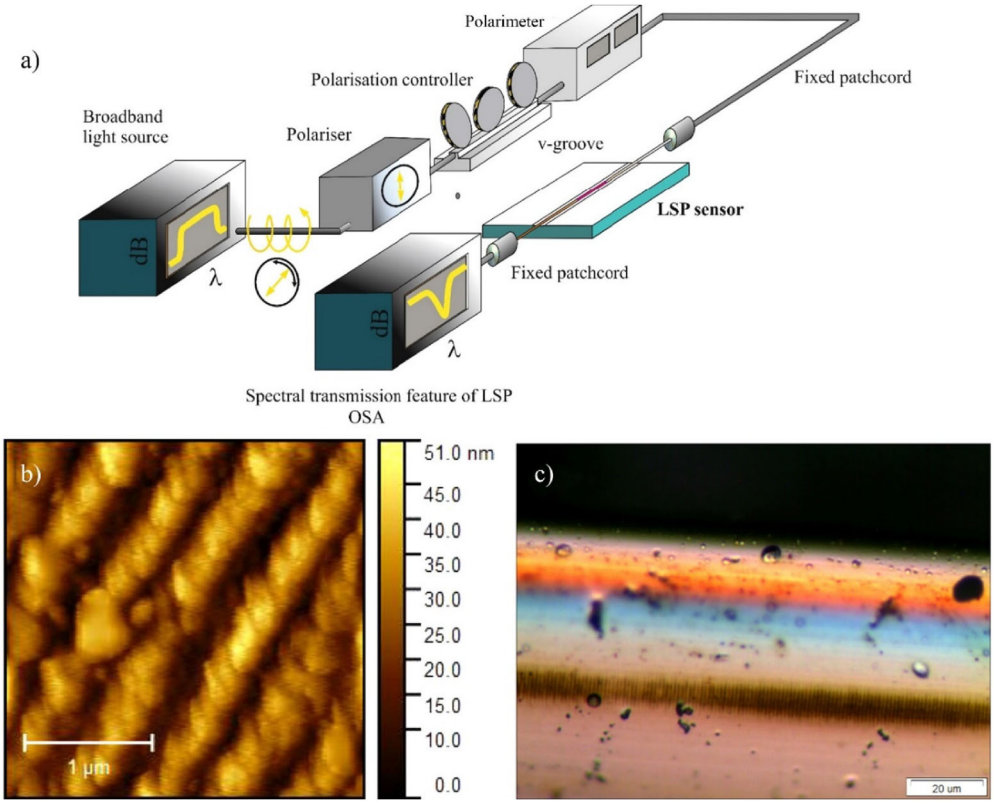

Figure 5. (a) Schematic representation of the LSP sensors platform (b) Surface profile of the LSP sensor (AFM image) (c) Optical microscope image of the plasmonic structure on the optical fiber.[7]

tested in real water samples.[139] In the recent PEC study, MoS_2/Ni-Fe layered double hydroxide (LDH) heterostructure and aptamer were used. Because of the nano-heterojunctions, MoS_2 showed optimal separation of photogenerated charge carriers and increased the visible-light absorption of NiFe-LDH. Using the change in the PEC signal because of the interaction between BPA and aptamer (Figure 6), a BPA sensor operating in the detection range of 0.22–43.8 pM and with a detection limit of 22.7 fM was developed.[140] The recovery of this platform in river water samples was 98.60–100.53%.

Another platform that provides successful analytical performance has been the field-effect transistor (FET). In this study using aptamer-modified multichannel carbon nanofibers (MCNFs), a detection limit of 1 fM was reported in the range of 1 fM–10 pM. FET platforms are known to provide successful detection limit values. However, no results related to real samples were given in this study.[100]

The contour chart was created by considering the analytical performance of the aptasensor platforms listed in Table 3 (Figure 7). For comparison purposes, the lower and upper limits of the operating range/linear range reported for the sensor are located on the x and y-axis (in log nM), while they are given on the z-axis in terms of LOD (log nM) obtained on that sensor platform.

As expected, it is seen that the sensor platforms show a diagonal distribution for the lower and upper detection range. It is also seen that contour lines are disturbed only on some sensor platforms. As seen in the contour chart, the relationship between the detection range (lower and upper limit) and the detection limit of the sensor platforms was maintained for most of the studies listed. This result demonstrates the detection range-detection limit dilemma in analytical studies. However, on some platforms, it was possible to both keep the detection range wider and lower the detection limit. These platforms are concentrated in areas that do not fit the general view (graph slope and parallelism of the checks) in the contour chart. Only a limited number of studies have overcome this analytical problem. However, the successful use of the listed studies in real samples is an inherent advantage of the selectivity of the aptamers. While the integration of the mediator into the aptamer provided successful results, especially in electrochemical structures, the integration of nanomaterials into platforms increased analytical performance in other platforms.

Comparison with other methods

We have seen that the analytical performance of aptamer-based sensor platforms is successful. But are aptamer platforms successful enough compared to other diagnostic element-bearing platforms? To get the answer to this question, we also discussed some of the BPA detection methods encountered in the literature in this section. Table 4 provides a comparative list of these different BPA detection sensor platforms. However, the specified list does not unfortunately include all studies. But we tried to include as many studies as possible for comparison.

First, when the electrochemical platforms are compared, it is seen that the mean log (LOD) value is 0.67 for the 12

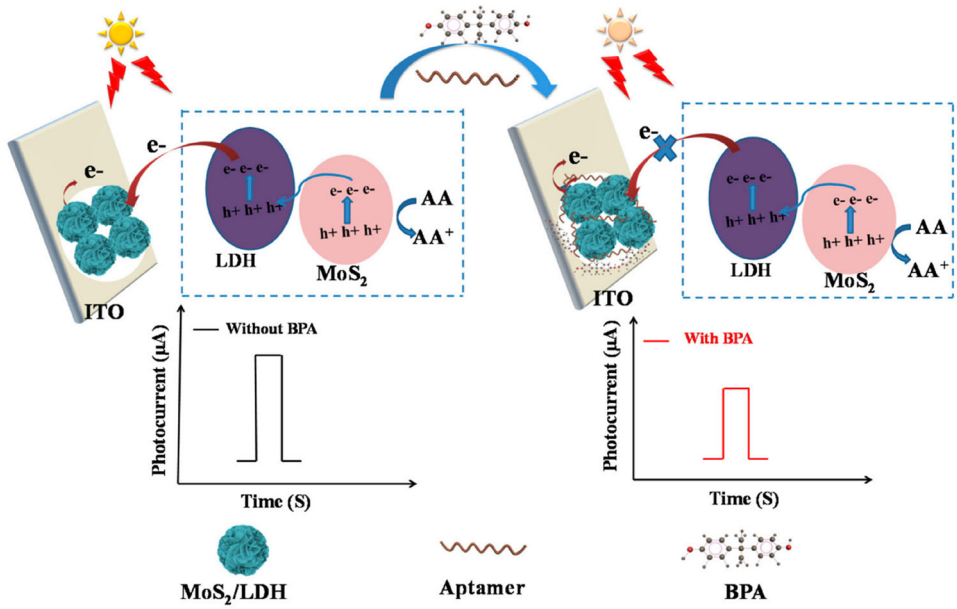

Figure 6. Mechanism of the PEC property based on aptamer/MoS_2/LDH-5% for BPA.[140]

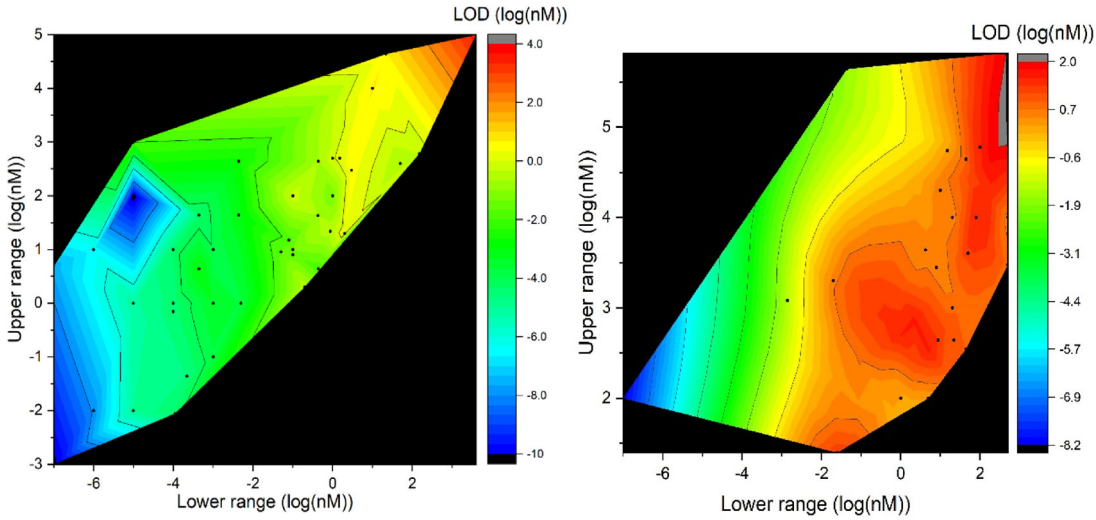

Figure 7. Contour plot of reviewed aptasensors listed in (a) Table 3 and (b) Table 4.

studies listed. This value is considerably higher than the mean log(LOD) value (−3.37) found for the electrochemical aptasensors listed in Table 3. However, this result is not sufficient to speculate, as there are numerous reports of aptamer-free BPA electrochemical sensors not included in this review article. We can group the electrochemical BPA sensors given in Table 4 as follows: enzymatic, molecularly imprinted polymers, and direct detection with electrode modification.

The detection limit in the range of 3–8 nM has been reported in enzymatic electrochemical sensor studies. Wu et al. provided a detection limit of 7.88 nM in the study using the Tyrosinase enzyme (Tyr), Au-Pt@SiO_2, Au decorated graphene, and GCE. 87.4–110.7% recovery was obtained with the real sample of olive oil chips.[156] In the enzymatic BPA detection performed by changing nanoparticles (biochar), this time on GCE, a detection limit of 3.18 nM was obtained, and the working range was 20 nM–10 μM.[157] A sensor using laccase and Ag-ZnO nanoparticles and MWCNTs on SPE provided a detection limit of 6 nM. The BPA recovery of this sensor from bottle samples was 89.3–109.3%.[160]

In the case of using molecularly imprinted polymers as a diagnostic element, successful sensors were obtained in terms of analytical performance. In two different studies using acetylene-black paste electrodes, different analytical performances were obtained with electrode modification. Deng et al. reported a LOD of 60 nM, while Xu et al. using graphene reported a LOD of 42 pM.[151,153] Both sensors were successfully used for BPA detection (max 5% RSD) in real samples (bottle, bag, packaging material, etc.). In two reports using GCE, the detection limit of 1.1 nM was decreased with AuNP,[155] while Ali et al. reported 8 nM LOD.[158] Although real samples were used in both studies, the real sample performance of the second study was low (∼30% RSD).

Table 4. Various BPA detection methods for comparison.

Method	Year	Approach	LOD	Linear range	Recovery %	Real samples	Ref.
Chemiluminescence	2019	DNAzyme-triggered chemiluminescence	5 nM	20 pM–2 μM	NR	NR	[147]
Colorimetric	2018	Hemin-functionalized rGO composites, peroxidase like activity	2 nM	5–100 nM	88.6–97.1	Tap water	[148]
Colorimetric	2018	Signal amplification via AuNP–antibody conjugates on poly amidoamine, lateral flow strip, immunosensor	44 nM	8.8–440 nM	NR	Buffer only	[149]
Colorimetric	2021	3′, 6′-bis(diethylamino)−2-((3,4,5 trimethyl benzylidene) amino)spiro [isoindoline-1,9′-xanthen] − 3-one chromophore conjugated with Fe^{3+}-ions	88 nM	0.44–660 μM	NR	Fish organs and bottle	[150]
Electrochemical	2011	Mg- Al-sodium dodecyl sulfate layered double hydroxide, GCE	2 nM	8 nM–2.8 μM	96.4–102.6	Tap water	[20]
Electrochemical	2013	ABPE electrode modified with a chitosan film, MIP	60 nM	0.08–10 μM	98.6–104.4	Bottle and bag	Deng[151]
Electrochemical	2013	Calf thymus DNA, single walled SWNT, nafion	5 nM	0.01–20 μM	94.0–106.0	Bottle	[152]
Electrochemical	2016	Acetylene-black paste electrode (ABPE), graphene, MIP	42 pM	1.4 pM–1.2 μM	95.4–102.6	Packaging material and water	[153]
Electrochemical	2016	Nitrogen-doped carbon nanofiber modified carbon paste electrode (CPE)	50 nM	0.1–60 μM	90.0–98.0	Water	[154]
Electrochemical	2017	AuNPs, MIP, GCE	1.1 nM	0.015–55 μM	97.6–106.5	Milk	[155]
Electrochemical	2019	Tyrosinase enzyme (Tyr), Au-Pt@SiO_2, Au decorated graphene, GCE	7.88 nM	0.044–44 μM	87.4–110.7	Olive oil chips	[156]
Electrochemical	2019	Biochar nanoparticles, Tyr enzyme, nafion, GCE	3.18 nM	0.02–10 μM	96.7–108.6	Water	[157]
Electrochemical	2019	Molecularly imprinted polymer (MIP), GCE	8 nM	0.02–1 μM	71.2–97.3	Tap water, drinking water	[158]
Electrochemical	2020	rGO, Fe_3O_4NPs, Trametes versicolor, GCE.	18.1 nM	25 pM–25 nM	107.0–124.0	Bottled water	[159]
Electrochemical	2020	Laccase, Ag-ZnONPs, MWCNTs, carbon screen printed electrode	6 nM	0.5–3.0 μM	89.3–109.3	Bottle	[160]
Electrochemical	2020	$CoFe_2O_4$ nanoparticle, GCE	3.6 nM	0.5–10 μM	95.5–102.0	Milk and tap water	[161]
Fluorescence	2015	Fluorescence polarization immunoassay (FPIA), 4,4-bis(4-hydroxyphenyl)-valeric acid − 4-(aminomethyl) uorescein	24.5 nM	0.05–4 μM	87.9–114.3	Water	[162]
Fluorescence	2016	Inner filter effect AuNPs on the fluorescence of CdTe quantum dots	8 nM	44–350 nM	NR	Water	[163]
Fluorescence	2019	Graphene quantum dots, MIP nanoparticle, nitrocelulose paper strip	4.38 nM	4.25 nM–4.38 μM	NR	Tap water and sea water	[164]
Fluorescence	2019	Signal amplification by activators generated by electron transfer for atom transfer radical polymerization	6.6 fM	100 fM–100 nM	91.1–122.5	Water	[165]
HPLC/fluorescence detector	2018	Samples were extracted ultrasonically with acetonitrile and cleaned using the QuEChERS technique	4.4 nM	21.9–438 nM	75.8–93.9	Milk	[166]
SERS	2016	Ag@Fe_2O_3 and Ag@Fe_2CoO_4 particles, aptamer, optofluidic chips patterned with magnetically activated nickel pads, SERS mapping	1 nM	∼1-100 nM	NR	NR	[167]
Surface Plasmon Resonance	2019	AuNPs, inhibition assay, immunosensor	22.8 pM	44 pM–438 μM	NR	Tap water	[168]

Successful analytical results have also been obtained with the integration of nanomaterials in electrochemical BPA sensors. Detection limits in the nM range were reported using $CoFe_2O_4$ nanoparticles,[161] reduced GO (rGO) and Fe_3O_4 nanoparticles,[159] and single-walled CNTs (SWCNTs) on the GCE electrode.[152] In these studies, BPA detection was also performed in real samples. In addition, the effect of electrode modifications on analytical performance was investigated and for this purpose, Mg-Al-sodium dodecyl sulfate layered double hydroxide coating[20] and nitrogen-doped carbon nanofiber modification[154] were used.

Fluorescent-based methods were also used to detect BPA. In these studies, in which aptamer was not used, selective BPA detection was aimed using immunoassay. Different strategies were used in studies included in high school and detection limits in the nM range were reported. A 24.5 nM LOD was reported in the fluorescence polarization immunoassay (FPIA) study using 4,4-bis(4-hydroxyphenyl)-valeric acid − 4-(aminomethyl) fluorescein.[162] This sensor platform provided 87.9–114.3% recovery in real water samples. Using the advantages of quantum dots, a detection limit of 8 nM was achieved with CdTe in the detection range of 44–350 nM.[163] In a study using graphene quantum dots and MIP as a diagnostic element, Uzek et al. developed a sensor platform with a detection limit of 4.38 nM and this platform was used for the detection of BPA in real water and seawater samples.[164]

In a study with high analytical performance among fluorescence-based studies, truncated BPA aptamer, click chemistry, and activators generated by electron transfer for atom transfer radical polymerization (AGET-ATRP) were used. The complementary DNA is conjugated with aminated magnetic beads through hydroxysuccinimide chemistry. Then, BPA-truncated aptamer (ssDNA-A) hybridizes with its

complementary single-stranded DNA (ssDNA-B) to form double-stranded DNA. In the presence of BPA, ssDNA-A specifically captures BPA to expose the azide group on magnetic beads. Then, the initiator (PBIB) is conjugated with an azide group of hairpins via the Cu(I)-catalyzed azide-alkyne cycloaddition (CuAAC). A large number of fluorescein molecules are introduced into the beads through the AGET-ATRP, which can amplify the signal of fluorescence dramatically. By this method, a detection limit of 6.6 fM is reported (100 fM–100 nM detection range). This platform was used to detect BPA in real samples with 91.1–122.5% recovery.[165]

Colorimetric approaches have also been used to detect BPA. Using hemin-functionalized rGO composites and peroxidase-like activity, 2 nM LOD,[148] 44 nM LOD with signal amplification via AuNP–antibody conjugates on poly amidoamine,[149] and 88 nM LOD with Fe^{3+}-ion conjugated chromophore were reported on these aptamer-free platforms.[150]

We also included several different approaches in Table 4 for comparison purposes. Among these, 5 nM LOD was reported with the DNAzyme-triggered chemiluminescence approach.[147] With the SERS platform using plasmonic nanoparticles, a detection limit of 1 nM was obtained in the detection range of 1–100 nM by using $Ag@Fe_2O_3$ and $Ag@Fe_2CoO_4$ nanoparticles for BPA detection.[167]

Another BPA detection approach that showed successful analytical performance in terms of detection limit was reported by Xue et al. This immunosensor based on surface plasmon resonance was used to detect BPA in a wide range from 44 pM to 438 µM using AuNPs and inhibition assay. The platform developed in this study, where a detection limit of 22.8 pM was obtained, was also used for the detection of BPA from tap water.[168]

Although we included the BPA detection method using a limited number of non-aptamer diagnostic elements in this review article, the contour chart was used to compare these studies with aptasensors (Figure 7(b)). In this chart, which provides an overview, it was seen that all analytical performance indicators (here only range and LOD) were worse compared to the aptasensors. Both the lower and upper values of the detection limit (x and y-axis) and the LOD (z-axis) values (logarithmically nM) are in a narrower range and higher compared to the aptasensors. However, it is not possible to use these results to prove the superiority of platforms carrying aptamer diagnostic elements. Instead, it can be concluded that sensor platforms using aptamer diagnostic elements are used as successfully in BPA detection as other platforms.

In general, the proposed sensor platforms for BPA detection have both analytical performance and high BPA detection performance in real samples. The reason why electrochemical sensors are studied more frequently in these platforms is probably the presence of BPA as a contaminant in environmental sources and that these environments cause interference in some platforms in terms of pH and ionic balance. However, in real sample experiments, it was also observed that the recovery values obtained using water and surface waters could not be obtained in more complex (such as wine, urine, or serum) matrices. Although it is known that the aptamers are minimally affected by the matrix as a diagnostic element, it is also seen that the recovery standard deviation values are >10% in some reports. This may be due to an incompatible combination of the diagnostic element and the sensor platform. Because it is often reported that aptamers give successful recovery values in much more complex matrices.

As a result, it is seen that the studies listed in Table 4 also give successful results in the detection of BPA from an analytical point of view. Among these platforms, the criteria that determine which platform is better are not clear. Therefore, only the detection limit, detection range, and actual sample analysis performances (if any) are compared in the comparison lists. For any sensor platform, this comparison is not adequate. However, other parameters such as ease of use, initial cost, and cost per analysis also form the criteria for the preferability of a sensor. At first glance, it can be said that the listed platforms do not make any obvious analytical performance difference, although it is assumed that the stated analytical performance criteria are sufficient to make a direct comparison. This was particularly evident in the PCA, where we compared (electrochemically) more studies.

Conclusion and future perspective

Detection of low-molecular contaminants such as BPA, from different environments, has always been challenging. This challenge exists even if biosensor platforms are used. This comprehensive review article on BPA detection is an example of sensor development studies that we will encounter with BPA analogs being classified as possible pollutants. Therefore, challenges are present not only for BPA but also for BPA derivatives of similar structure and size. The detection limit of about 44 nM and a wide recovery rate obtained with ELISA kits for BPA detection can be considered an analytical benchmark. Thus, nearly all BPA detection platforms covered in this review article appear to meet or exceed this analytical performance.

However, the diagnostic element for BPA is discussed in this review article. Generally, immunosensors are insufficient due to poor immunogenicity, especially using low molecular weight pollutants as antigens to immunized animals. On the other hand, it is seen that the use of aptamers provides an advantage in the detection of pollutants such as BPA. For this reason, different sensor platforms with aptamer diagnostic elements have been reported in the detection of BPA with increasing studies in the last decade. Inherent advantages of aptamers have also been the reason for preference in these studies. Aptamers are very versatile and are least likely to be affected by matrix-dependent parameters such as pH or ionic charge in the detection of a contaminant in water or different environmental samples.

Considering the reports discussed in this study, it is seen that electrochemical platforms are frequently studied as BPA aptasensors and exhibit successful analytical performance. It was seen that different amplification approaches yield

results. Among these, the integration of nanomaterials into the sensor platform and the attachment of the mediator as a label to the aptamer or another conjugate oligonucleotide sequence come to the fore. Similar integrations have yielded results in PEC and plasmonic platforms.

However, the bottleneck of the studies discussed in this review article is that an aptamer developed for BPA is used mostly and the aptamer obtained by truncation of this aptamer is used several times. An alternative diagnostic element has not been developed yet and studies in the literature are based on the use of the same diagnostic element with different strategies. This resulted in real sample test results with almost similar recovery % across all runs. It can be thought that another aptamer sequence with higher selectivity will further increase analytical performances in BPA detection. At this point, difficulties might arise in selecting high-affinity aptamers for the detection of such small molecules with SELEX. However, this seems to be a surmountable problem because of combining in silico aptamer selection methods with different SELEX protocols.

When considered in terms of signal amplification strategies, it is seen that different approaches have been tried in BPA detection. It can be thought that the limitation at this stage is not to increase the analysis cost. Because BPA detection does not require a very low detection limit and a very wide working range, especially considering the current migration/residual limit values. However, regulatory organizations are creating new working groups for both BPA and BPA analogs and evaluating the status of the pollutant. For this reason, it should not be thought that stricter limit values will not be introduced. In this case, we can predict that different amplification strategies (even if the cost increases) will be applied. Another challenge is the need for continuous on-site analysis. For an environmental pollutant such as BPA, the area of use of sensors is specific. Continuous measurement is a necessity in these areas. Therefore, it is necessary to focus on miniaturization and reusability studies.

In this review article, we also showed that statistical evaluation can be made when we have enough study results. However, although it seems to be a wide distribution, we have seen that the values we define as analytical performance indicators do not create very different clusters in PCA. However, we explained why some of the studies that left the list had a better analytical performance. We hope that similar statistical approaches will be used in future review articles. It was seen that aptamers are successfully utilized in the detection of low molecular mass and common pollutants (or pollutant candidates) such as BPA. It was also determined that a wide detection limit was obtained between the different signal amplification strategies and aM-nM. It would not be wrong to say that with the selection of new aptamers, many new reports will be brought to the literature in the detection of BPA and, most importantly, BPA analogs.

ORCID

Samet Şahin http://orcid.org/0000-0002-0568-4283

References

[1] Zhang, Y.; Lei, Y.; Lu, H.; Shi, L.; Wang, P.; Ali, Z.; Li, J. Electrochemical Detection of Bisphenols in Food: A Review. *Food Chem.* **2021**, *346*, 128895.

[2] Sofen, L. E.; Furst, A. L. Perspective – Electrochemical Sensors to Monitor Endocrine Disrupting Pollutants. *J. Electrochem. Soc.* **2020**, *167*, 037524. DOI: 10.1149/2.0242003JES.

[3] Kang, J.-H.; Kondo, F.; Katayama, Y. Human Exposure to Bisphenol A. *Toxicology* **2006**, *226*, 79–89. DOI: 10.1016/j.tox.2006.06.009.

[4] Zhang, W.; Liu, Q.; Lin, J. Prevention from the Pollution of Carcinogenic Endocrine Disrupting Chemicals in Water Sources. *Cancer Prev. Curr. Res.* **2017**, *1*, 111.

[5] Bergman, A.; Heindel, J. J.; Kasten, T.; Kidd, K. A.; Jobling, S.; Neira, M.; Zoeller, R. T.; Becher, G.; Bjerregaard, P.; Bornman, R.; et al. The İmpact of Endocrine Disruption: A Consensus Statement on the State of the Science. *Environ. Health Perspect.* **2013**, *121*, A104–6.

[6] Plahuta, M.; Tišler, T.; Toman, M. J.; Pintar, A. Toxic and Endocrine Disrupting Effects of Wastewater Treatment Plant İnfluents and Effluents on a Freshwater İsopod Asellus Aquaticus (Isopoda, Crustacea). *Chemosphere* **2017**, *174*, 342–353. DOI: 10.1016/j.chemosphere.2017.01.137.

[7] Allsop, T. D. P.; Neal, R.; Wang, C.; Nagel, D. A.; Hine, A. V.; Culverhouse, P.; Ania Castañón, J. D.; Webb, D. J.; Scarano, S.; Minunni, M.; et al. An Ultra-Sensitive Aptasensor on Optical Fibre for the Direct Detection of Bisphenol A. *Biosens. Bioelectron.* **2019**, *135*, 102–110. DOI: 10.1016/j.bios.2019.02.043.

[8] Lichnovský, J.; et al. Contamination of Potentially Toxic Elements in Streams and Water Sediments in the Area of Abandoned Pb-Zn-Cu Deposits (Hrubý Jesenník, Czech Republic). *IOP Conf. Ser: Earth Environ. Sci.* **2017**, *92*, 012037.

[9] Nguyen, V.-T.; Kwon, Y. S.; Gu, M. B. Aptamer-Based Environmental Biosensors for Small Molecule Contaminants. *Curr. Opin. Biotechnol.* **2017**, *45*, 15–23. DOI: 10.1016/j.copbio.2016.11.020.

[10] Rochester, J. R. Bisphenol A and Human Health: A Review of the Literature. *Reprod. Toxicol.* **2013**, *42*, 132–155. DOI: 10.1016/j.reprotox.2013.08.008.

[11] Rosenmai, A. K.; Dybdahl, M.; Pedersen, M.; Alice van Vugt-Lussenburg, B. M.; Wedebye, E. B.; Taxvig, C.; Vinggaard, A. M. Are Structural Analogues to Bisphenol A Safe Alternatives? *Toxicol. Sci.* **2014**, *139*, 35–47. DOI: 10.1093/toxsci/kfu030.

[12] Zhu, W.; Yue, X.; Duan, J.; Zhang, Y.; Zhang, W.; Yu, S.; Wang, Y.; Zhang, D.; Wang, J. Electrochemically co-Reduced 3D GO-C60 Nanoassembly as an Efficient Nanocatalyst for Electrochemical Detection of Bisphenol S. *Electrochim. Acta* **2016**, *188*, 85–90. DOI: 10.1016/j.electacta.2015.11.131.

[13] Yang, J.; Wang, X.; Zhang, D.; Wang, L.; Li, Q.; Zhang, L. Simultaneous Determination of Endocrine Disrupting Compounds Bisphenol F and Bisphenol AF Using Carboxyl Functionalized Multi-Walled Carbon Nanotubes Modified Electrode. *Talanta.* **2014**, *130*, 207–212. DOI: 10.1016/j.talanta.2014.06.056.

[14] Wang, X.; Yang, L.; Jin, X.; Zhang, L. Electrochemical Determination of Estrogenic Compound Bisphenol F in Food Packaging Using Carboxyl Functionalized Multi-Walled Carbon Nanotubes Modified Glassy Carbon Electrode. *Food Chem.* **2014**, *157*, 464–469. DOI: 10.1016/j.foodchem.2014.02.079.

[15] Chen, D.; Kannan, K.; Tan, H.; Zheng, Z.; Feng, Y.-L.; Wu, Y.; Widelka, M. Bisphenol Analogues Other Than BPA: Environmental Occurrence, Human Exposure, and Toxicity—A Review. *Environ. Sci. Technol.* **2016**, *50*, 5438–5453. DOI: 10.1021/acs.est.5b05387.

[16] Rochester, J. R.; Bolden, A. L. Bisphenol S and F: A Systematic Review and Comparison of the Hormonal Activity of

Bisphenol A Substitutes. *Environ. Health Perspect.* **2015**, *123*, 643–650. DOI: 10.1289/ehp.1408989.

[17] Cabaton, N.; Dumont, C.; Severin, I.; Perdu, E.; Zalko, D.; Cherkaoui-Malki, M.; Chagnon, M.-C. Genotoxic and Endocrine Activities of Bis(Hydroxyphenyl)Methane (Bisphenol F) and İts Derivatives in the HepG2 Cell Line. *Toxicology* **2009**, *255*, 15–24. DOI: 10.1016/j.tox.2008.09.024.

[18] Stossi, F.; Bolt, M. J.; Ashcroft, F. J.; Lamerdin, J. E.; Melnick, J. S.; Powell, R. T.; Dandekar, R. D.; Mancini, M. G.; Walker, C. L.; Westwick, J. K.; et al. Defining Estrogenic Mechanisms of Bisphenol A Analogs through High Throughput Microscopy-Based Contextual Assays. *Chem. Biol.* **2014**, *21*, 743–753. DOI: 10.1016/j.chembiol.2014.03.013.

[19] Sinha, A.; Wu, L.; Lu, X.; Chen, J.; Jain, R. Advances in Sensing and Biosensing of Bisphenols: A Review. *Anal Chim Acta* **2018**, *998*, 1–27. DOI: 10.1016/j.aca.2017.09.048.

[20] Yin, H.; Zhou, Y.; Cui, L.; Liu, X.; Ai, S.; Zhu, L. Electrochemical Oxidation Behavior of Bisphenol A at Surfactant/Layered Double Hydroxide Modified Glassy Carbon Electrode and İts Determination. *J. Solid State Electrochem.* **2011**, *15*, 167–173. DOI: 10.1007/s10008-010-1089-6.

[21] Erler, C.; Novak, J. Bisphenol A Exposure: Human Risk and Health Policy. *J. Pediatr. Nurs.* **2010**, *25*, 400–407. DOI: 10.1016/j.pedn.2009.05.006.

[22] Organization, W. H. Joint FAO/WHO expert meeting to review toxicological and health aspects of bisphenol A: summary report including report of stakeholder meeting on bisphenol A. World Health Organization, **2010**. http://www.who.int/foodsafety/chem/chemicals/BPA_Summary2010.pdf. [accessed 11 March 2011].

[23] Diamanti-Kandarakis, E.; Bourguignon, J.-P.; Giudice, L. C.; Hauser, R.; Prins, G. S.; Soto, A. M.; Zoeller, R. T.; Gore, A. C. Endocrine-Disrupting Chemicals: an Endocrine Society Scientific Statement. *Endocr. Rev.* **2009**, *30*, 293–342. DOI: 10.1210/er.2009-0002.

[24] Chen, S.; Chang, Q.; Yin, K.; He, Q.; Deng, Y.; Chen, B.; Liu, C.; Wang, Y.; Wang, L. Rapid Analysis of Bisphenol A and Its Analogues in Food Packaging Products by Paper Spray Ionization Mass Spectrometry. *J. Agric. Food Chem.* **2017**, *65*, 4859–4865. DOI: 10.1021/acs.jafc.7b02061.

[25] Schönfelder, G.; Wittfoht, W.; Hopp, H.; Talsness, C. E.; Paul, M.; Chahoud, I. Parent Bisphenol A Accumulation in the Human Maternal-Fetal-Placental Unit. *Environ. Health Perspect.* **2002**, *110*, A703–7. DOI: 10.1289/ehp.021100703.

[26] Toppari, J.; Larsen, J. C.; Christiansen, P.; Giwercman, A.; Grandjean, P.; Guillette, L. J.; Jégou, B.; Jensen, T. K.; Jouannet, P.; Keiding, N.; et al. Male Reproductive Health and Environmental Xenoestrogens. *Environ. Health Perspect.* **1996**, *104*, 741–803. DOI: 10.1289/ehp.96104s4741.

[27] Vandenberg, L. N.; Hauser, R.; Marcus, M.; Olea, N.; Welshons, W. V. Human Exposure to Bisphenol A (BPA). *Reprod. Toxicol.* **2007**, *24*, 139–177. DOI: 10.1016/j.reprotox.2007.07.010.

[28] Segner, H.; Caroll, K.; Fenske, M.; Janssen, C. R.; Maack, G.; Pascoe, D.; Schäfers, C.; Vandenbergh, G. F.; Watts, M.; Wenzel, A.; et al. Identification of Endocrine-Disrupting Effects in Aquatic Vertebrates and İnvertebrates: Report from the European IDEA Project. *Ecotoxicol. Environ. Saf.* **2003**, *54*, 302–314. DOI: 10.1016/S0147-6513(02)00039-8.

[29] Oppeneer, S. J.; Robien, K. Bisphenol A Exposure and Associations with Obesity among Adults: A Critical Review. *Public Health Nutr.* **2015**, *18*, 1847–1863. DOI: 10.1017/S1368980014002213.

[30] Huo, X.; Chen, D.; He, Y.; Zhu, W.; Zhou, W.; Zhang, J. Bisphenol-a and Female İnfertility: A Possible Role of Gene-Environment İnteractions. *Int. J. Environ. Res. Public Health.* **2015**, *12*, 11101–11116. DOI: 10.3390/ijerph120911101.

[31] Flint, S.; Markle, T.; Thompson, S.; Wallace, E. Bisphenol A Exposure, Effects, and Policy: A Wildlife Perspective. *J. Environ. Manage.* **2012**, *104*, 19–34. DOI: 10.1016/j.jenvman.2012.03.021.

[32] Watabe, Y.; Kondo, T.; Morita, M.; Tanaka, N.; Haginaka, J.; Hosoya, K. Determination of Bisphenol A in Environmental Water at Ultra-Low Level by High-Performance Liquid Chromatography with an Effective on-Line Pretreatment Device. *J. Chromatogr. A* **2004**, *1032*, 45–49. DOI: 10.1016/j.chroma.2003.11.079.

[33] Vogel, S. A. The Politics of Plastics: The Making and Unmaking of Bisphenol a "Safety". *Am. J. Public Health.* **2009**, *99*, S559–S566. DOI: 10.2105/AJPH.2008.159228.

[34] Michałowicz, J. Bisphenol A – Sources, Toxicity and Biotransformation. *Environ. Toxicol. Pharmacol.* **2014**, *37*, 738–758. DOI: 10.1016/j.etap.2014.02.003.

[35] Arnold, S. M.; Clark, K. E.; Staples, C. A.; Klecka, G. M.; Dimond, S. S.; Caspers, N.; Hentges, S. G. Relevance of Drinking Water as a Source of Human Exposure to Bisphenol A. *J. Expo. Sci. Environ. Epidemiol.* **2013**, *23*, 137–144. DOI: 10.1038/jes.2012.66.

[36] Razavipanah, I.; Rounaghi, G. H.; Deiminiat, B.; Damirchi, S.; Abnous, K.; Izadyar, M.; Khavani, M. A New Electrochemical Aptasensor Based on MWCNT-SiO 2 @Au Core-Shell Nanocomposite for Ultrasensitive Detection of Bisphenol A. *Microchem. J.* **2019**, *146*, 1054–1063. DOI: 10.1016/j.microc.2019.02.018.

[37] Ensafi, A. A.; Amini, M.; Rezaei, B. Molecularly İmprinted Electrochemical Aptasensor for the Attomolar Detection of Bisphenol A. *Microchim. Acta* **2018**, *185*, 265. DOI: 10.1007/s00604-018-2810-x.

[38] Noureddine El Moussawi, S.; Ouaini, R.; Matta, J.; Chébib, H.; Cladière, M.; Camel, V. Simultaneous Migration of Bisphenol Compounds and Trace Metals in Canned Vegetable Food. *Food Chem.* **2019**, *288*, 228–238. DOI: 10.1016/j.foodchem.2019.02.116.

[39] Fürhacker, M.; Scharf, S.; Weber, H. Bisphenol A: Emissions from Point Sources. *Chemosphere.* **2000**, *41*, 751–756. DOI: 10.1016/S0045-6535(99)00466-X.

[40] Bolz, U.; Hagenmaier, H.; Körner, W. Phenolic Xenoestrogens in Surface Water, Sediments, and Sewage Sludge from Baden-Württemberg, South-West Germany. *Environ. Pollut.* **2001**, *115*, 291–301. DOI: 10.1016/S0269-7491(01)00100-2.

[41] Heemken, O. P.; Reincke, H.; Stachel, B.; Theobald, N. The Occurrence of Xenoestrogens in the Elbe River and the North Sea. *Chemosphere.* **2001**, *45*, 245–259. DOI: 10.1016/S0045-6535(00)00570-1.

[42] Fromme, H.; Küchler, T.; Otto, T.; Pilz, K.; Müller, J.; Wenzel, A. Occurrence of Phthalates and Bisphenol A and F in the Environment. *Water Res.* **2002**, *36*, 1429–1438. DOI: 10.1016/S0043-1354(01)00367-0.

[43] Kleywegt, S.; Pileggi, V.; Yang, P.; Hao, C.; Zhao, X.; Rocks, C.; Thach, S.; Cheung, P.; Whitehead, B. Pharmaceuticals, Hormones and Bisphenol A in Untreated Source and Finished Drinking Water in Ontario, Canada–Occurrence and Treatment Efficiency. *Sci. Total Environ.* **2011**, *409*, 1481–1488. DOI: 10.1016/j.scitotenv.2011.01.010.

[44] Klecka, G. M.; Staples, C. A.; Clark, K. E.; Van der Hoeven, N.; Thomas, D. E.; Hentges, S. G. Exposure Analysis of Bisphenol A in Surface Water Systems in North America and Europe. *Environ. Sci. Technol.* **2009**, *43*, 6145–6150.

[45] Snyder, S. A. Occurrence, Treatment, and Toxicological Relevance of EDCs and Pharmaceuticals in Water. *Ozone Sci. Eng.* **2008**, *30*, 65–69. DOI: 10.1080/01919510701799278.

[46] Peyre, L.; Rouimi, P.; de Sousa, G.; Héliès-Toussaint, C.; Carré, B.; Barcellini, S.; Chagnon, M.-C.; Rahmani, R. Comparative Study of Bisphenol A and İts Analogue Bisphenol S on Human Hepatic Cells: A Focus on Their Potential İnvolvement in Nonalcoholic Fatty Liver Disease. *Food Chem. Toxicol.* **2014**, *70*, 9–18. DOI: 10.1016/j.fct.2014.04.011.

[47] Sui, Y.; Ai, N.; Park, S.-H.; Rios-Pilier, J.; Perkins, J. T.; Welsh, W. J.; Zhou, C. Bisphenol A and İts Analogues Activate Human Pregnane X Receptor. *Environ. Health Perspect.* **2012**, *120*, 399–405. DOI: 10.1289/ehp.1104426.

[48] Peng, Y.; Wang, J.; Wu, C. Determination of Endocrine Disruption Potential of Bisphenol A Alternatives in Food Contact Materials Using in Vitro Assays: State of the Art and Future Challenges. *J. Agric. Food Chem.* **2019**, *67*, 12613–12625. DOI: 10.1021/acs.jafc.9b01543.

[49] Liang, X.; Yin, N.; Liang, S.; Yang, R.; Liu, S.; Lu, Y.; Jiang, L.; Zhou, Q.; Jiang, G.; Faiola, F.; et al. Bisphenol A and Several Derivatives Exert Neural Toxicity in Human Neuron-like Cells by Decreasing Neurite Length. *Food Chem. Toxicol.* **2020**, *135*, 111015. DOI: 10.1016/j.fct.2019.111015.

[50] Thoene, M.; Dzika, E.; Gonkowski, S.; Wojtkiewicz, J. Bisphenol S in Food Causes Hormonal and Obesogenic Effects Comparable to or Worse than Bisphenol a: A Literature Review. *Nutrients* **2020**, *12*, 532. DOI: 10.3390/nu12020532.

[51] Kim, J.-J.; Kumar, S.; Kumar, V.; Lee, Y.-M.; Kim, Y.-S.; Kumar, V. Bisphenols as a Legacy Pollutant, and Their Effects on Organ Vulnerability. *IJERPH.* **2019**, *17*, 112. DOI: 10.3390/ijerph17010112.

[52] Santoro, A.; Chianese, R.; Troisi, J.; Richards, S.; Nori, S. L.; Fasano, S.; Guida, M.; Plunk, E.; Viggiano, A.; Pierantoni, R.; et al. Neuro-Toxic and Reproductive Effects of BPA. *Curr. Neuropharmacol.* **2019**, *17*, 1109–1132. DOI: 10.2174/1570159X17666190726112101.

[53] Liu, B.; Lehmler, H.-J.; Sun, Y.; Xu, G.; Liu, Y.; Zong, G.; Sun, Q.; Hu, F. B.; Wallace, R. B.; Bao, W.; et al. Bisphenol A Substitutes and Obesity in US Adults: analysis of a Population-Based, Cross-Sectional Study. *Lancet. Planet. Health.* **2017**, *1*, e114–e122. DOI: 10.1016/S2542-5196(17)30049-9.

[54] Chin, K. Y.; Pang, K. L.; Mark-Lee, W. F. A Review on the Effects of Bisphenol a and İts Derivatives on Skeletal Health. *Int. J. Med. Sci.* **2018**, *15*, 1043–1050. DOI: 10.7150/ijms.25634.

[55] Grumetto, L.; Gennari, O.; Montesano, D.; Ferracane, R.; Ritieni, A.; Albrizio, S.; Barbato, F. Determination of Five Bisphenols in Commercial Milk Samples by Liquid Chromatography Coupled to Fluorescence Detection. *J. Food Prot.* **2013**, *76*, 1590–1596. DOI: 10.4315/0362-028X.JFP-13-054.

[56] Stuart, J. D.; Capulong, C. P.; Launer, K. D.; Pan, X. Analyses of Phenolic Endocrine Disrupting Chemicals in Marine Samples by Both Gas and Liquid Chromatography-Mass Spectrometry. *J. Chromatogr. A* **2005**, *1079*, 136–145. DOI: 10.1016/j.chroma.2005.03.075.

[57] Alnaimat, A. S.; Barciela-Alonso, M. C.; Bermejo-Barrera, P. Determination of Bisphenol A in Tea Samples by Solid Phase Extraction and Liquid Chromatography Coupled to Mass Spectrometry. *Microchem. J.* **2019**, *147*, 598–604. DOI: 10.1016/j.microc.2019.03.026.

[58] Sun, F.; Kang, L.; Xiang, X.; Li, H.; Luo, X.; Luo, R.; Lu, C.; Peng, X. Recent Advances and Progress in the Detection of Bisphenol A. *Anal. Bioanal. Chem.* **2016**, *408*, 6913–6927. DOI: 10.1007/s00216-016-9791-6.

[59] Moriyama, K.; Tagami, T.; Akamizu, T.; Usui, T.; Saijo, M.; Kanamoto, N.; Hataya, Y.; Shimatsu, A.; Kuzuya, H.; Nakao, K.; et al. Thyroid Hormone Action is Disrupted by Bisphenol A as an Antagonist. *J. Clin. Endocrinol. Metab.* **2002**, *87*, 5185–5190. DOI: 10.1210/jc.2002-020209.

[60] Fukata, H.; Miyagawa, H.; Yamazaki, N.; Mori, C. Comparison of Elisa- and LC-MS-Based Methodologies for the Exposure Assessment of Bisphenol A. *Toxicol. Mech. Methods.* **2006**, *16*, 427–430. DOI: 10.1080/15376520600697404.

[61] Sheng, W.; Duan, W.; Shi, Y.; Chang, Q.; Zhang, Y.; Lu, Y.; Wang, S. Sensitive Detection of Bisphenol A in Drinking Water and River Water Using an Upconversion Nanoparticles-Based Fluorescence İmmunoassay in Combination with Magnetic Separation. *Anal. Methods* **2018**, *10*, 5313–5320. DOI: 10.1039/C8AY01260A.

[62] Gugoasa, L. A. D. Review – Electrochemical Sensors for Determination of the Endocrine Disruptor. *J. Electrochem. Soc.* **2020**, *167*, 037506. DOI: 10.1149/2.0062003JES.

[63] Ragavan, K. V.; Rastogi, N. K.; Thakur, M. S. Sensors and Biosensors for Analysis of bisphenol-A. *TrAC Trend Anal Chem.* **2013**, *52*, 248–260. DOI: 10.1016/j.trac.2013.09.006.

[64] Mei, Z.; Chu, H.; Chen, W.; Xue, F.; Liu, J.; Xu, H.; Zhang, R.; Zheng, L. Ultrasensitive One-Step Rapid Visual Detection of Bisphenol A in Water Samples by Label-Free Aptasensor. *Biosens. Bioelectron.* **2013**, *39*, 26–30. DOI: 10.1016/j.bios.2012.06.027.

[65] Varmira, K.; Saed-Mocheshi, M.; Jalalvand, A. R. Electrochemical Sensing and Bio-Sensing of Bisphenol A and Detection of İts Damage to DNA: A Comprehensive Review. *Sens. Bio-Sens. Res.* **2017**, *15*, 17–33. DOI: 10.1016/j.sbsr.2017.07.002.

[66] Marchesini, G. R.; Meulenberg, E.; Haasnoot, W.; Irth, H. Biosensor İmmunoassays for the Detection of Bisphenol A. *Anal. Chim. Acta* **2005**, *528*, 37–45. DOI: 10.1016/j.aca.2004.06.066.

[67] Freymuth, F.; Quibriac, M.; Petitjean, J.; Amiel, M. L.; Pothier, P.; Denis, A.; Duhamel, J. F. Comparison of Two New Tests for Rapid Diagnosis of Respiratory Syncytial Virus İnfections by Enzyme-Linked İmmunosorbent Assay and İmmunofluorescence Techniques. *J. Clin. Microbiol.* **1986**, *24*, 1013–1016. DOI: 10.1128/jcm.24.6.1013-1016.1986.

[68] Zheng, J.; Zhang, K.; Zhao, S. Q. [Study on Spectral and İmmune İdentification of Artificial Antigen of Bisphenol A]. *Guang Pu Xue Yu Guang Pu Fen Xi* **2008**, *28*, 1583–1586.

[69] Tuerk, C.; Gold, L. Systematic Evolution of Ligands by Exponential Enrichment: RNA Ligands to Bacteriophage T4 DNA Polymerase. *Science* **1990**, *249*, 505–510. DOI: 10.1126/science.2200121.

[70] Ellington, A. D.; Szostak, J. W. In Vitro Selection of RNA Molecules That Bind Specific Ligands. *Nature* **1990**, *346*, 818–822. DOI: 10.1038/346818a0.

[71] Gold, L.; et al. From oligonucleotide shapes to genomic SELEX: Novel biological regulatory loops. *Proc Nation Acad Sci.* **1997**, *94*, p. 59–64.

[72] Jenison, R. D.; Gill, S. C.; Pardi, A.; Polisky, B. High-Resolution Molecular Discrimination by RNA. *Science* **1994**, *263*, 1425–1429. DOI: 10.1126/science.7510417.

[73] Sheedy, C.; MacKenzie, C. R.; Hall, J. C. Isolation and Affinity Maturation of Hapten-Specific Antibodies. *Biotechnol. Adv.* **2007**, *25*, 333–352. DOI: 10.1016/j.biotechadv.2007.02.003.

[74] Mirzajani, H.; Cheng, C.; Wu, J.; Chen, J.; Eda, S.; Najafi Aghdam, E.; Badri Ghavifekr, H. A Highly Sensitive and Specific Capacitive Aptasensor for Rapid and Label-Free Trace Analysis of Bisphenol A (BPA) in Canned Foods. *Biosens. Bioelectron.* **2017**, *89*, 1059–1067. DOI: 10.1016/j.bios.2016.09.109.

[75] Yu, Z.; Luan, Y.; Li, H.; Wang, W.; Wang, X.; Zhang, Q. A Disposable Electrochemical Aptasensor Using Single-Stranded DNA–Methylene Blue Complex as Signal-Amplification Platform for Sensitive Sensing of Bisphenol A. *Sens. Actuator. B: Chem.* **2019**, *284*, 73–80. DOI: 10.1016/j.snb.2018.12.126.

[76] Geiger, A.; Burgstaller, P.; von der Eltz, H.; Roeder, A.; Famulok, M. RNA Aptamers That Bind L-Arginine with Sub-Micromolar Dissociation Constants and High Enantioselectivity. *Nucleic Acids Res.* **1996**, *24*, 1029–1036. DOI: 10.1093/nar/24.6.1029.

[77] Giamberardino, A.; Labib, M.; Hassan, E. M.; Tetro, J. A.; Springthorpe, S.; Sattar, S. A.; Berezovski, M. V.; DeRosa, M. C. Ultrasensitive Norovirus Detection Using DNA Aptasensor Technology. *PLoS One.* **2013**, *8*, e79087. DOI: 10.1371/journal.pone.0079087.

[78] Akki, S. U.; Werth, C. J.; Silverman, S. K. Selective Aptamers for Detection of Estradiol and Ethynylestradiol in Natural

Waters. *Environ. Sci. Technol.* **2015**, *49*, 9905–9913. DOI: 10.1021/acs.est.5b02401.
[79] Jayasena, S. D. Aptamers: an Emerging Class of Molecules That Rival Antibodies in Diagnostics. *Clin. Chem.* **1999**, *45*, 1628–1650. DOI: 10.1093/clinchem/45.9.1628.
[80] McKeague, M.; Bradley, C. R.; De Girolamo, A.; Visconti, A.; Miller, J. D.; Derosa, M. C. Screening and Initial Binding Assessment of Fumonisin B1 Aptamers. *Int. J. Mol. Sci.* **2010**, *11*, 4864–4881. DOI: 10.3390/ijms11124864.
[81] Niazi, J. H.; Lee, S. J.; Gu, M. Single-Stranded DNA Aptamers Specific for Antibiotics Tetracyclines. *Bioorg. Med. Chem.* **2008**, *16*, 7245–7253. DOI: 10.1016/j.bmc.2008.06.033.
[82] Stoltenburg, R.; Reinemann, C.; Strehlitz, B. FluMag-SELEX as an Advantageous Method for DNA Aptamer Selection. *Anal. Bioanal. Chem.* **2005**, *383*, 83–91. DOI: 10.1007/s00216-005-3388-9.
[83] Mendonsa, S. D.; Bowser, M. T. In Vitro Evolution of Functional DNA Using Capillary Electrophoresis. *J. Am. Chem. Soc.* **2004**, *126*, 20–21. DOI: 10.1021/ja037832s.
[84] Yang, J.; Bowser, M. T. Capillary Electrophoresis–SELEX Selection of Catalytic DNA Aptamers for a Small-Molecule Porphyrin Target. *Anal. Chem.* **2013**, *85*, 1525–1530. DOI: 10.1021/ac302721j.
[85] Park, J.-W.; Tatavarty, R.; Kim, D. W.; Jung, H.-T.; Gu, M. B. Immobilization-Free Screening of Aptamers Assisted by Graphene Oxide. *Chem Commun (Camb).* **2012**, *48*, 2071–2073. DOI: 10.1039/c2cc16473f.
[86] Lee, E.-H.; Lim, H. J.; Lee, S.-D.; Son, A. Highly Sensitive Detection of Bisphenol A by NanoAptamer Assay with Truncated Aptamer. *ACS Appl. Mater. Interfaces.* **2017**, *9*, 14889–14898. DOI: 10.1021/acsami.7b02377.
[87] Huang, L.; Yang, X.; Qi, C.; Niu, X.; Zhao, C.; Zhao, X.; Shangguan, D.; Yang, Y. A Label-Free Electrochemical Biosensor Based on a DNA Aptamer against Codeine. *Anal. Chim. Acta.* **2013**, *787*, 203–210. DOI: 10.1016/j.aca.2013.05.024.
[88] Gu, H.; Duan, N.; Wu, S.; Hao, L.; Xia, Y.; Ma, X.; Wang, Z. Graphene Oxide-Assisted Non-İmmobilized SELEX of Okdaic Acid Aptamer and the Analytical Application of Aptasensor. *Sci. Rep.* **2016**, *6*, 21665. DOI: 10.1038/srep21665.
[89] Mei, H.; Bing, T.; Yang, X.; Qi, C.; Chang, T.; Liu, X.; Cao, Z.; Shangguan, D. Functional-Group Specific Aptamers İndirectly Recognizing Compounds with Alkyl Amino Group. *Anal. Chem.* **2012**, *84*, 7323–7329. DOI: 10.1021/ac300281u.
[90] Jo, M.; Ahn, J.-Y.; Lee, J.; Lee, S.; Hong, S. W.; Yoo, J.-W.; Kang, J.; Dua, P.; Lee, D.-K.; Hong, S.; et al. Development of Single-Stranded DNA Aptamers for Specific Bisphenol a Detection. *Oligonucleotides.* **2011**, *21*, 85–91. DOI: 10.1089/oli.2010.0267.
[91] Zuker, M. Mfold Web Server for Nucleic Acid Folding and Hybridization Prediction. *Nucleic Acids Res.* **2003**, *31*, 3406–3415. DOI: 10.1093/nar/gkg595.
[92] Zhang, D.; Yang, J.; Ye, J.; Xu, L.; Xu, H.; Zhan, S.; Xia, B.; Wang, L. Colorimetric Detection of Bisphenol A Based on Unmodified Aptamer and Cationic Polymer Aggregated Gold Nanoparticles. *Anal. Biochem.* **2016**, *499*, 51–56. DOI: 10.1016/j.ab.2016.01.011.
[93] Verdian-Doghaei, A.; Housaindokht, M. R.; Abnous, K. A Fluorescent Aptasensor for Potassium İon Detection-Based Triple-Helix Molecular Switch. *Anal. Biochem.* **2014**, *466*, 72–75. DOI: 10.1016/j.ab.2014.08.014.
[94] Lim, H. J.; Chua, B.; Son, A. Detection of Bisphenol A Using Palm-Size NanoAptamer Analyzer. *Biosens. Bioelectron.* **2017**, *94*, 10–18. DOI: 10.1016/j.bios.2017.02.029.
[95] Chen, J.; Zhou, S. Label-Free DNA Y Junction for Bisphenol A Monitoring Using Exonuclease III-Based Signal Protection Strategy. *Biosens. Bioelectron.* **2016**, *77*, 277–283. DOI: 10.1016/j.bios.2015.09.042.
[96] Hu, L.-Y.; Niu, C.-G.; Wang, X.-Y.; Huang, D.-W.; Zhang, L.; Zeng, G.-M. Magnetic Separate "Turn-on" Fluorescent Biosensor for Bisphenol A Based on Magnetic Oxidation Graphene. *Talanta.* **2017**, *168*, 196–202. DOI: 10.1016/j.talanta.2017.03.055.
[97] Beiranvand, Z. S.; Abbasi, A. R.; Dehdashtian, S.; Karimi, Z.; Azadbakht, A. Aptamer-Based Electrochemical Biosensor by Using Au-Pt Nanoparticles, Carbon Nanotubes and Acriflavine Platform. *Anal. Biochem.* **2017**, *518*, 35–45. DOI: 10.1016/j.ab.2016.10.001.
[98] Abnous, K.; Danesh, N. M.; Ramezani, M.; Alibolandi, M.; Taghdisi, S. M. A Novel Electrochemical Sensor for Bisphenol A Detection Based on Nontarget-İnduced Extension of Aptamer Length and Formation of a Physical Barrier. *Biosens. Bioelectron.* **2018**, *119*, 204–208. DOI: 10.1016/j.bios.2018.08.024.
[99] Derikvandi, Z.; Abbasi, A. R.; Roushani, M.; Derikvand, Z.; Azadbakht, A. Design of Ultrasensitive Bisphenol A–Aptamer Based on Platinum Nanoparticles Loading to Polyethyleneimine-Functionalized Carbon Nanotubes. *Anal. Biochem.* **2016**, *512*, 47–57. DOI: 10.1016/j.ab.2016.06.007.
[100] Kim, S. G.; Lee, J. S.; Jun, J.; Shin, D. H.; Jang, J. Ultrasensitive Bisphenol A Field-Effect Transistor Sensor Using an Aptamer-Modified Multichannel Carbon Nanofiber Transducer. *ACS Appl. Mater. Interfaces.* **2016**, *8*, 6602–6610. DOI: 10.1021/acsami.5b11159.
[101] Ma, Y.; Liu, J.; Li, H. Diamond-Based Electrochemical Aptasensor Realizing a Femtomolar Detection Limit of Bisphenol A. *Biosens. Bioelectron.* **2017**, *92*, 21–25. DOI: 10.1016/j.bios.2017.01.041.
[102] Zhang, Y.; Cao, T.; Huang, X.; Liu, M.; Shi, H.; Zhao, G. A Visible-Light Driven Photoelectrochemical Aptasensor for Endocrine Disrupting Chemicals Bisphenol A with High Sensitivity and Specificity. *Electroanalysis.* **2013**, *25*, 1787–1795. DOI: 10.1002/elan.201300057.
[103] Guo, X.; Wu, S.; Duan, N.; Wang, Z. Mn2+-Doped NaYF4:Yb/Er Upconversion Nanoparticle-Based Electrochemiluminescent Aptasensor for Bisphenol A. *Anal. Bioanal. Chem.* **2016**, *408*, 3823–3831. DOI: 10.1007/s00216-016-9470-7.
[104] Chung, E.; Jeon, J.; Yu, J.; Lee, C.; Choo, J. Surface-Enhanced Raman Scattering Aptasensor for Ultrasensitive Trace Analysis of Bisphenol A. *Biosens. Bioelectron.* **2015**, *64*, 560–565. DOI: 10.1016/j.bios.2014.09.087.
[105] Alsager, O. A.; Kumar, S.; Hodgkiss, J. M. Lateral Flow Aptasensor for Small Molecule Targets Exploiting Adsorption and Desorption Interactions on Gold Nanoparticles. *Anal. Chem.* **2017**, *89*, 7416–7424. DOI: 10.1021/acs.analchem.7b00906.
[106] Cui, H.; Wu, J.; Eda, S.; Chen, J.; Chen, W.; Zheng, L. Rapid Capacitive Detection of Femtomolar Levels of Bisphenol A Using an Aptamer-Modified Disposable Microelectrode Array. *Microchim. Acta.* **2015**, *182*, 2361–2367. DOI: 10.1007/s00604-015-1556-y.
[107] Zhu, Y.; Zhou, C.; Yan, X.; Yan, Y.; Wang, Q. Aptamer-Functionalized Nanoporous Gold Film for High-Performance Direct Electrochemical Detection of Bisphenol A in Human Serum. *Anal. Chim. Acta.* **2015**, *883*, 81–89. DOI: 10.1016/j.aca.2015.05.002.
[108] Zhou, L.; Wang, J.; Li, D.; Li, Y. An Electrochemical Aptasensor Based on Gold Nanoparticles Dotted Graphene Modified Glassy Carbon Electrode for Label-Free Detection of Bisphenol A in Milk Samples. *Food Chem.* **2014**, *162*, 34–40. DOI: 10.1016/j.foodchem.2014.04.058.
[109] Kashefi-Kheyrabadi, L.; Kim, J.; Gwak, H.; Hyun, K.-A.; Bae, N. H.; Lee, S. J.; Jung, H.-I. A Microfluidic Electrochemical Aptasensor for Enrichment and Detection of Bisphenol A. *Biosens. Bioelectron.* **2018**, *117*, 457–463. DOI: 10.1016/j.bios.2018.06.036.
[110] Li, X.; Song, J.; Xue, Q.-W.; You, F.-H.; Lu, X.; Kong, Y.-C.; Ma, S.-Y.; Jiang, W.; Li, C.-Z. A Label-Free and Sensitive Fluorescent Qualitative Assay for Bisphenol A Based on

Rolling Circle Amplification/Exonuclease III-Combined Cascade Amplification. *Nanomaterials.* **2016**, *6*, 190. DOI: 10.3390/nano6100190.

[111] Zhu, Y.; Cai, Y.; Xu, L.; Zheng, L.; Wang, L.; Qi, B.; Xu, C. Building an Aptamer/Graphene Oxide FRET Biosensor for One-Step Detection of Bisphenol A. *ACS Appl. Mater. Interfaces.* **2015**, *7*, 7492–7496. DOI: 10.1021/acsami.5b00199.

[112] Feng, J.; Xu, L.; Cui, G.; Wu, X.; Ma, W.; Kuang, H.; Xu, C. Building SERS-Active Heteroassemblies for Ultrasensitive Bisphenol A Detection. *Biosens. Bioelectron.* **2016**, *81*, 138–142. DOI: 10.1016/j.bios.2016.02.055.

[113] Lin, X.; Cheng, C.; Terry, P.; Chen, J.; Cui, H.; Wu, J. Rapid and Sensitive Detection of Bisphenol a from Serum Matrix. *Biosens. Bioelectron.* **2017**, *91*, 104–109. DOI: 10.1016/j.bios.2016.12.024.

[114] Xu, J.; Li, Y.; Bie, J.; Jiang, W.; Guo, J.; Luo, Y.; Shen, F.; Sun, C. Colorimetric Method for Determination of Bisphenol A Based on Aptamer-Mediated Aggregation of Positively Charged Gold Nanoparticles. *Microchim. Acta.* **2015**, *182*, 2131–2138. DOI: 10.1007/s00604-015-1547-z.

[115] Zhu, Y.; Gu, X.; Jiang, F.; Jia, R.; Jin, M.; Chen, M.; Zhang, G. Ultrasensitive Detection of Bisphenol A Based on an Aptasensor with DNA Amplification. *Food Agric. Immunol.* **2018**, *29*, 1106–1115. DOI: 10.1080/09540105.2018.1515893.

[116] Kang, B.; Kim, J. H.; Kim, S.; Yoo, K.-H. Aptamer-Modified Anodized Aluminum Oxide-Based Capacitive Sensor for the Detection of Bisphenol A. *Appl. Phys. Lett.* **2011**, *98*, 073703. DOI: 10.1063/1.3555345.

[117] Xue, F.; Wu, J.; Chu, H.; Mei, Z.; Ye, Y.; Liu, J.; Zhang, R.; Peng, C.; Zheng, L.; Chen, W.; et al. Electrochemical Aptasensor for the Determination of Bisphenol A in Drinking Water. *Microchim. Acta.* **2013**, *180*, 109–115. DOI: 10.1007/s00604-012-0909-z.

[118] Yu, P.; Liu, Y.; Zhang, X.; Zhou, J.; Xiong, E.; Li, X.; Chen, J. A Novel Electrochemical Aptasensor for Bisphenol A Assay Based on Triple-Signaling Strategy. *Biosens. Bioelectron.* **2016**, *79*, 22–28. DOI: 10.1016/j.bios.2015.12.007.

[119] Kazane, I.; Gorgy, K.; Gondran, C.; Spinelli, N.; Zazoua, A.; Defrancq, E.; Cosnier, S. Highly Sensitive Bisphenol-A Electrochemical Aptasensor Based on Poly(Pyrrole-Nitrilotriacetic Acid)-Aptamer. *Anal. Chem.* **2016**, *88*, 7268–7273. DOI: 10.1021/acs.analchem.6b01574.

[120] Liu, Y. J.; Liu, Y.; Liu, B. H. A Dual-Signaling Strategy for Ultrasensitive Detection of Bisphenol A by Aptamer-Based Electrochemical Biosensor. *Electroanal. Chem.* **2016**, *781*, 265–271. DOI: 10.1016/j.jelechem.2016.06.048.

[121] Azadbakht, A.; Roushani, M.; Abbasi, A. R.; Derikvand, Z. A Novel İmpedimetric Aptasensor, Based on Functionalized Carbon Nanotubes and Prussian Blue as Labels. *Anal. Biochem.* **2016**, *512*, 58–69. DOI: 10.1016/j.ab.2016.08.006.

[122] Cheng, C.; Wang, S.; Wu, J.; Yu, Y.; Li, R.; Eda, S.; Chen, J.; Feng, G.; Lawrie, B.; Hu, A.; et al. Bisphenol A Sensors on Polyimide Fabricated by Laser Direct Writing for Onsite River Water Monitoring at Attomolar Concentration. *ACS Appl. Mater. Interfaces.* **2016**, *8*, 17784–17792. DOI: 10.1021/acsami.6b03743.

[123] Deiminiat, B.; Rounaghi, G. H.; Arbab-Zavar, M. H.; Razavipanah, I. A Novel Electrochemical Aptasensor Based on f-MWCNTs/AuNPs Nanocomposite for Label-Free Detection of Bisphenol A. *Sens. Actuator. B: Chem.* **2017**, *242*, 158–166. DOI: 10.1016/j.snb.2016.11.041.

[124] Baghayeri, M.; Ansari, R.; Nodehi, M.; Razavipanah, I.; Veisi, H. Voltammetric Aptasensor for Bisphenol A Based on the Use of a MWCNT/Fe3O4@Gold Nanocomposite. *Microchim. Acta.* **2018**, *185*, 320. DOI: 10.1007/s00604-018-2838-y.

[125] Shi, L.; Rong, X.; Wang, Y.; Ding, S.; Tang, W. High-Performance and Versatile Electrochemical Aptasensor Based on Self-Supported Nanoporous Gold Microelectrode and Enzyme-İnduced Signal Amplification. *Biosens. Bioelectron.* **2018**, *102*, 41–48. DOI: 10.1016/j.bios.2017.11.012.

[126] Li, H.; Ding, S.; Wang, W.; Lv, Q.; Wang, Z.; Bai, H.; Zhang, Q. Voltammetric Aptasensor for Bisphenol A Based on Double Signal Amplification via Gold-Coated Multiwalled Carbon Nanotubes and an ssDNA–Dye Complex. *Microchim. Acta.* **2019**, *186*, 860. DOI: 10.1007/s00604-019-4006-4.

[127] Li, M.; Guo, Z.; Zheng, X.; Yang, H.; Feng, W.; Kong, J. An Electrochemical Aptasensor Based on eATRP Amplification for the Detection of Bisphenol A. *Analyst.* **2019**, *144*, 5691–5699. DOI: 10.1039/c9an01266d.

[128] Nazari, M.; Kashanian, S.; Rafipour, R.; Omidfar, K. Biosensor Design Using an Electroactive Label-Based Aptamer to Detect Bisphenol A in Serum Samples. *J. Biosci.* **2019**, *44*, 105. DOI: 10.1007/s12038-019-9921-3.

[129] Hassani, S.; Rezaei Akmal, M.; Salek Maghsoudi, A.; Rahmani, S.; Vakhshiteh, F.; Norouzi, P.; Ganjali, M. R.; Abdollahi, M. High-Performance Voltammetric Aptasensing Platform for Ultrasensitive Detection of Bisphenol A as an Environmental Pollutant. *Front. Bioeng. Biotechnol.* **2020**, *8*, 574846. DOI: 10.3389/fbioe.2020.574846.

[130] Baghayeri, M.; Amiri, A.; Fayazi, M.; Nodehi, M.; Esmaeelnia, A. Electrochemical Detection of Bisphenol a on a MWCNTs/CuFe2O4 Nanocomposite Modified Glassy Carbon Electrode. *Mater. Chem. Phys.* **2021**, *261*, 124247. DOI: 10.1016/j.matchemphys.2021.124247.

[131] Chen, C. F.; Li, D.; Jin, B. K. Development of a Selective Electrochemical Biosensor for Bisphenol a Based on Target-Induced Chain Release Involving Methylene Blue Release. *Anal. Lett.* **2022**, *55*, 1782–1796. DOI: 10.1080/00032719.2022.2026374.

[132] Cao, H.-X.; Wang, L.; Pan, C.-G.; He, Y.-S.; Liang, G.-X. Aptamer Based Electrochemiluminescent Determination of Bisphenol A by Using Carboxylated Graphitic Carbon Nitride. *Mikrochim. Acta.* **2018**, *185*, 463. DOI: 10.1007/s00604-018-2997-x.

[133] Ragavan, K. V.; Selvakumar, L. S.; Thakur, M. S. Functionalized Aptamers as Nano-Bioprobes for Ultrasensitive Detection of bisphenol-A. *Chem. Commun. (Camb).* **2013**, *49*, 5960–5962. DOI: 10.1039/c3cc42002g.

[134] Ribes, À.; Aznar, E.; Bernardos, A.; Marcos, M. D.; Amorós, P.; Martínez-Máñez, R.; Sancenón, F. Fluorogenic Sensing of Carcinogenic Bisphenol A Using Aptamer-Capped Mesoporous Silica Nanoparticles. *Chemistry.* **2017**, *23*, 8581–8584. DOI: 10.1002/chem.201701024.

[135] He, M.-Q.; Wang, K.; Wang, J.; Yu, Y.-L.; He, R.-H. A Sensitive Aptasensor Based on Molybdenum Carbide Nanotubes and Label-Free Aptamer for Detection of Bisphenol A. *Anal. Bioanal. Chem.* **2017**, *409*, 1797–1803. DOI: 10.1007/s00216-016-0123-7.

[136] Xu, Z.; Chen, Y.; Tang, Y.; Chen, M.; Chen, W.; Cheng, Y. Aptamer-Enhanced Fluorescence Determination of Bisphenol A after Magnetic Solid-Phase Extraction Using Fe3O4@SiO2@Aptamer. *Anal. Methods.* **2020**, *12*, 4479–4486. DOI: 10.1039/d0ay01124j.

[137] Su, Y.; Shao, C.; Huang, X.; Qi, J.; Ge, R.; Guan, H.; Lin, Z. Extraction and Detection of Bisphenol A in Human Serum and Urine by Aptamer-Functionalized Magnetic Nanoparticles. *Anal. Bioanal. Chem.* **2018**, *410*, 1885–1891. DOI: 10.1007/s00216-017-0801-0.

[138] Kuang, H.; Yin, H.; Liu, L.; Xu, L.; Ma, W.; Xu, C. Asymmetric Plasmonic Aptasensor for Sensitive Detection of Bisphenol A. *ACS Appl. Mater. Interfaces.* **2014**, *6*, 364–369. DOI: 10.1021/am4043678.

[139] Jiang, D.; Du, X.; Zhou, L.; Li, H.; Wang, K. TiO2 Nanoparticles Embedded in Borocarbonitrides Nanosheets for Sensitive and Selective Photoelectrochemical Aptasensing of Bisphenol A. *Electroanal. Chem.* **2018**, *818*, 191–197. DOI: 10.1016/j.jelechem.2018.04.042.

[140] Gao, H.; He, Y.; Liu, J. New Aptamer/MoS2/Ni-Fe LDH Photoelectric Sensor for Bisphenol A Determination. *Nanomaterials.* **2021**, *12*, 78. DOI: 10.3390/nano12010078.

[141] Marks, H. L.; Pishko, M. V.; Jackson, G. W.; Coté, G. L. Rational Design of a Bisphenol A Aptamer Selective Surface-Enhanced Raman Scattering Nanoprobe. *Anal. Chem.* **2014**, *86*, 11614–11619. DOI: 10.1021/ac502541v.

[142] Wang, C.-Y.; Zeng, Y.; Shen, A.-G.; Hu, J.-M. A Highly Sensitive SERS Probe for Bisphenol A Detection Based on Functionalized Au@Ag Nanoparticles. *Anal. Methods.* **2018**, *10*, 5622–5628. DOI: 10.1039/C8AY01966E.

[143] Schiano, M. E.; Abduvakhidov, A.; Varra, M.; Albrizio, S. Aptamer-Based Biosensors for the Analytical Determination of Bisphenol A in Foodstuffs. *Appl. Sci.* **2022**, *12*, 3752. DOI: 10.3390/app12083752.

[144] Rajabnejad, S.-H.; Badibostan, H.; Verdian, A.; Karimi, G. R.; Fooladi, E.; Feizy, J. Aptasensors as Promising New Tools in Bisphenol A detection – An İnvisible Pollution in Food and Environment. *Microchem. J.* **2020**, *155*, 104722. DOI: 10.1016/j.microc.2020.104722.

[145] Acharya, P. B.; George, A.; Shrivastav, P. S. A Status Update on the Development of Polymer and Metal-Based Graphene Electrochemical Sensors for Detection and Quantitation of Bisphenol A. *Crit. Rev. Anal. Chem.* **2022**, 1–22. DOI: 10.1080/10408347.2022.2094197.

[146] Lee, E.-S.; Kim, G. B.; Ryu, S.-H.; Kim, H.; Yoo, H. H.; Yoon, M. Y.; Lee, J.-W.; Gye, M. C.; Kim, Y.-P. Fluorescing Aptamer-Gold Nanosensors for Enhanced Sensitivity to Bisphenol A. *Sens. Actuator. B: Chem.* **2018**, *260*, 371–379. DOI: 10.1016/j.snb.2018.01.018.

[147] Xu, J.; Lee, E.-S.; Gye, M. C.; Kim, Y.-P. Rapid and Sensitive Determination of Bisphenol A Using Aptamer and Split DNAzyme. *Chemosphere.* **2019**, *228*, 110–116. DOI: 10.1016/j.chemosphere.2019.04.110.

[148] Xiong, Z.; Zhong, H.; Zheng, S.; Deng, P.; Li, N.; Yun, W.; Yang, L. A Visual Detection of Bisphenol A Based on Peroxidase-like Activity of Hemin–Graphene Composites and Aptamer. *Anal. Methods.* **2018**, *10*, 2450–2455. DOI: 10.1039/C8AY00677F.

[149] Peng, X.; Kang, L.; Pang, F.; Li, H.; Luo, R.; Luo, X.; Sun, F. A Signal-Enhanced Lateral Flow Strip Biosensor for Ultrasensitive and on-Site Detection of Bisphenol A. *Food Agric. Immunol.* **2018**, *29*, 216–227. DOI: 10.1080/09540105.2017.1365822.

[150] Sundaram, E.; Manna, A.; Lakshmi Servarayan, K.; Sivasamy Vasantha, V. Colorimetric Detection and Bio-Magnification of Bisphenol A in Fish Organs and Water Sources Using 3′,6′-Bis(Diethylamino)-2-((3,4,5trimethyl Benzylidene) Amino) Spiro İsoindoline-1,9′-Xanthen -3-One (BTSIXO)-Fe3+ İon Conjugate. *Food Chem.* **2021**, *345*, 128627. DOI: 10.1016/j.foodchem.2020.128627.

[151] Deng, P.; Xu, Z.; Li, J.; Kuang, Y. Acetylene Black Paste Electrode Modified with a Molecularly İmprinted Chitosan Film for the Detection of Bisphenol A. *Microchim. Acta.* **2013**, *180*, 861–869. DOI: 10.1007/s00604-013-1001-z.

[152] Jiang, X.; Ding, W.; Luan, C.; Ma, Q.; Guo, Z. Biosensor for Bisphenol A Leaching from Baby Bottles Using a Glassy Carbon Electrode Modified with DNA and Single Walled Carbon Nanotubes. *Microchim. Acta.* **2013**, *180*, 1021–1028. DOI: 10.1007/s00604-013-1025-4.

[153] Xu, W.; Yuan, F.; Li, C.; Huang, W.; Wu, X.; Yin, Z.; Yang, W. Acetylene Black Paste Electrode Modified with Molecularly İmprinted Polymers/Graphene for the Determination of Bisphenol A. *J. Sep. Sci.* **2016**, *39*, 4851–4857. DOI: 10.1002/jssc.201600803.

[154] Sun, J.; Liu, Y.; Lv, S.; Huang, Z.; Cui, L.; Wu, T. An Electrochemical Sensor Based on Nitrogen-Doped Carbon Nanofiber for Bisphenol A Determination. *Electroanalysis.* **2016**, *28*, 439–444. DOI: 10.1002/elan.201500287.

[155] Zhao, W.-R.; Kang, T.-F.; Lu, L.-P.; Shen, F.-X.; Cheng, S.-Y. A Novel Electrochemical Sensor Based on Gold Nanoparticles and Molecularly İmprinted Polymer with Binary Functional Monomers for Sensitive Detection of Bisphenol A. *Electroanal. Chem.* **2017**, *786*, 102–111. DOI: 10.1016/j.jelechem.2017.01.003.

[156] Wu, L.; Yan, H.; Wang, J.; Liu, G.; Xie, W. Tyrosinase İncorporated with Au-Pt@SiO2 Nanospheres for Electrochemical Detection of Bisphenol A. *J. Electrochem. Soc.* **2019**, *166*, B562–B568. DOI: 10.1149/2.0141908jes.

[157] Liu, Y.; Yao, L.; He, L.; Liu, N.; Piao, Y. Electrochemical Enzyme Biosensor Bearing Biochar Nanoparticle as Signal Enhancer for Bisphenol a Detection in Water. *Sensors (Switzerland).* **2019**, *19*, 1619. DOI: 10.3390/s19071619.

[158] Ali, H.; Mukhopadhyay, S.; Jana, N. R. Selective Electrochemical Detection of Bisphenol A Using a Molecularly İmprinted Polymer Nanocomposite. *New J. Chem.* **2019**, *43*, 1536–1543. DOI: 10.1039/C8NJ05883K.

[159] Fernandes, P. M. V.; Campiña, J. M.; Silva, A. F. A Layered Nanocomposite of Laccase, Chitosan, and Fe3O4 Nanoparticles-Reduced Graphene Oxide for the Nanomolar Electrochemical Detection of Bisphenol A. *Microchim. Acta.* **2020**, *187*, 262. DOI: 10.1007/s00604-020-4223-x.

[160] Kunene, K.; Sabela, M.; Kanchi, S.; Bisetty, K. High Performance Electrochemical Biosensor for Bisphenol A Using Screen Printed Electrodes Modified with Multiwalled Carbon Nanotubes Functionalized with Silver-Doped Zinc Oxide. *Waste Biomass Valor.* **2020**, *11*, 1085–1096. DOI: 10.1007/s12649-018-0505-5.

[161] Liu, Q.; Kang, X.; Xing, L.; Ye, Z.; Yang, Y. A Facile Synthesis of Nanostructured CoFe2O4 for the Electrochemical Sensing of Bisphenol A. *RSC Adv.* **2020**, *10*, 6156–6162. DOI: 10.1039/c9ra10936f.

[162] Huang, P.; Zhao, S.; Eremin, S. A.; Zheng, S.; Lai, D.; Chen, Y.; Guo, B. A Fluorescence Polarization İmmunoassay Method for Detection of the Bisphenol A Residue in Environmental Water Samples Based on a Monoclonal Antibody and 4′-(Aminomethyl)Fluorescein. *Anal. Methods* **2015**, *7*, 4246–4251. DOI: 10.1039/C5AY00818B.

[163] Li, Y.; Xu, J.; Wang, L.; Huang, Y.; Guo, J.; Cao, X.; Shen, F.; Luo, Y.; Sun, C. Aptamer-Based Fluorescent Detection of Bisphenol A Using Nonconjugated Gold Nanoparticles and CdTe Quantum Dots. *Sens. Actuators, B* **2016**, *222*, 815–822. DOI: 10.1016/j.snb.2015.08.130.

[164] Uzek, R.; et al. A Nitrocellulose Paper Strip for Fluorometric Determination of Bisphenol A Using Molecularly Imprinted Nanoparticles. *Microchim. Acta.* **2019**, *186*, 218. DOI: 10.1007/s00604-019-3323-y.

[165] Guo, Z.; Tang, J.; Li, M.; Liu, Y.; Yang, H.; Kong, J. An Ultrasensitive Fluorescent Aptasensor Based on Truncated Aptamer and AGET ATRP for the Detection of Bisphenol A. *Anal. Bioanal. Chem.* **2019**, *411*, 7807–7815. DOI: 10.1007/s00216-019-02179-1.

[166] Xiong, L.; Yan, P.; Chu, M.; Gao, Y.-Q.; Li, W.-H.; Yang, X.-L. A Rapid and Simple HPLC-FLD Screening Method with QuEChERS as the Sample Treatment for the Simultaneous Monitoring of Nine Bisphenols in Milk. *Food Chem.* **2018**, *244*, 371–377. DOI: 10.1016/j.foodchem.2017.10.030.

[167] Marks, H.; Huang, P.-J.; Mabbott, S.; Graham, D.; Kameoka, J.; Coté, G. Ferric Plasmonic Nanoparticles, Aptamers, and Magnetofluidic Chips: Toward the Development of Diagnostic Surface-Enhanced Raman Spectroscopy Assays. *J. Biomed. Opt.* **2016**, *21*, 127005. DOI: 10.1117/1.JBO.21.12.127005.

[168] Xue, C. S.; Erika, G.; Jiří, H. Surface Plasmon Resonance Biosensor for the Ultrasensitive Detection of Bisphenol A. *Anal. Bioanal. Chem.* **2019**, *411*, 5655–5658. DOI: 10.1007/s00216-019-01996-8.